MRI Techniques for Noninvasive Monitoring of Transplanted Organs

José M. F. Moura

Students: Charnchai Pluempitiwiriyawej, Y. Sun, Hsun-Hsien Chang

Pittsburgh NMR Center for Biomedical Research
Dept. of Electrical and Computer Engineering
Carnegie Mellon University, Pittsburgh, PA, USA

Siemens Corporate Research
Princeton NJ
July 31/ 2003

Support by NIH (grants R01EB/AI-00318 and P41RR-03631)

Outline

- MRI at CMU
- Goals of research:
  - Monitoring transplanted organ function
    - Automatic segmentation
    - Organ function
- Transplanted organs in animal models:
  - Kidneys
  - Heart

Centers with Bioimaging Interests

**Structural Biology Pr.
(CMU)**

**Center Neural Basis of Cognition
(CMU/PITT)**

**MR Res. Center
(UPMC)**

**Brain Trauma Res. Ct.
(UPMC)**

**Sensor Tech. Center
(CMU)**

**Pittsburgh NMR Center
(CMU/PITT)**

**3-T fMRI Brain Imaging Center
(CMU/PITT)**

NMR Center for Biomedical Research

- Founded in 1986, NIH funded since 1988
- 1 of 7 NIH NCRR Biomedical Research Resource Centers for NMR MRI/ MRS – now through NBIB
- Only one exclusively devoted to small animal models
- 8400 sq. ft. facility at Mellon Institute
- Jointly administered by CMU/ Pitt
- Director: Prof. Chien Ho (Biological Sc.)
- Renewed September 1st/ 2003-August 31st/ 2008

NMR Center

- NMR Center: MRI and MRS instruments
  - 1 Brucker 11.7 T, 8.9 cm vertical bore (microimaging small animal mice, high resolution)
  - 2 Brucker Avance DRX (4.7 T and 7.0 T) MRI/MRS
  - Home-built 2.35 T MRI/MRS
  - Brucker Minispec .47 T NMR Instrument
  - 4 High resolution multinuclear NMR spectrometers (300, 500, 600 MHz)
  - All equipped with gradient capability
- Animal research:
  - Surgical and physiological monitoring equipment (microscopes, pumps, ventilators, electrocautery, gas analyzers, …)
- Computing and data processing facilities

Goals

- **Scientific Goal** — **Noninvasive MRI Methodology for Early Detection of Organ Malfunction**

  { ***Transplanted*** **organs – early detection of rejection**
  Kidney **and** ***heart*** **small animal models**

- **Research Goal** — **Signal/Image Processing Alg. for** ***Automatic*** **Detection of Organ Malfunction**
- **Task 1:** — **Automatic organ segmentation**
- **Task 2:** — **Automatic detection of organ rejection**

Challenges: low contrast, clutter, missing edge info.

Kidneys

Track the dynamic behavior of the transplanted organ

Automatic segmentation of kidneys & their internal structures

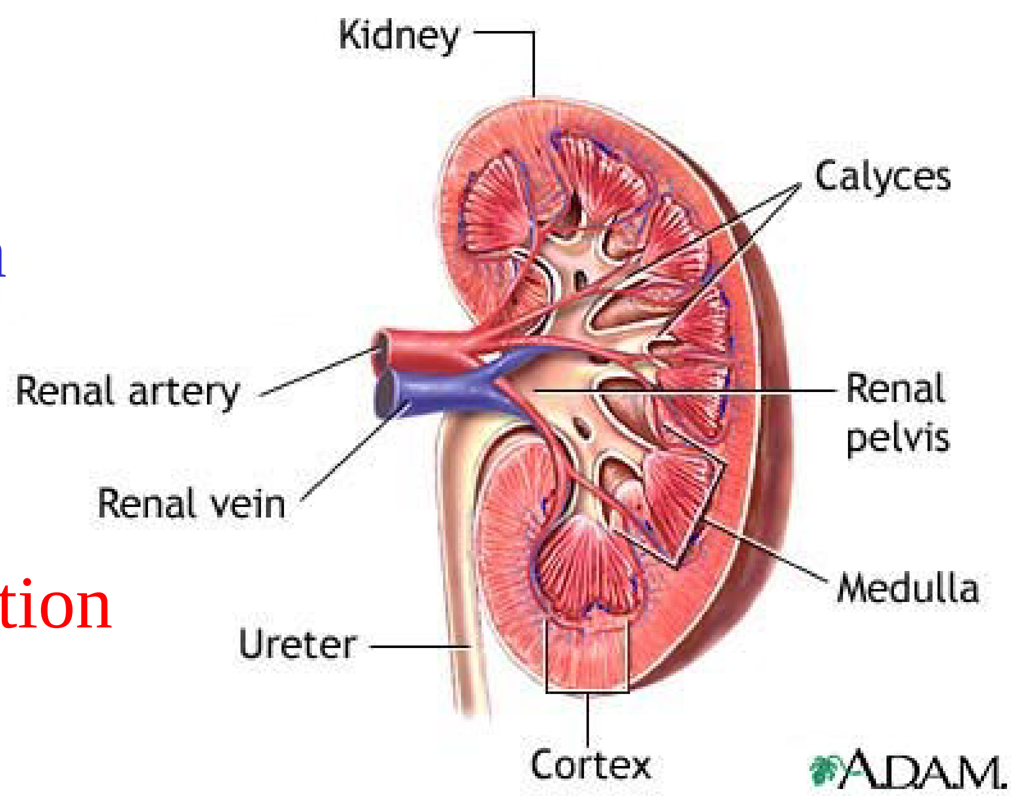

Block Diagram of Kidney Segmentation Algorithm

g → Movement Correction and Noise Reduction → f → Kidney Segmentation → Segmentation of Cortex and Medulla

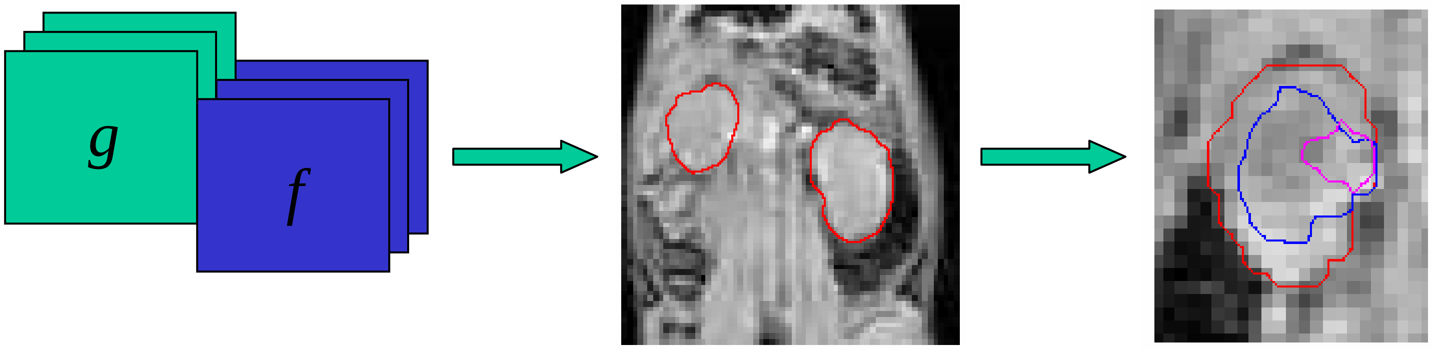

MRI Data

USPIO enhanced dynamic MRI: ultra-small superparamagnetic iron oxide

(6 mg Fe/kg body weight)

Groups of rats

a. Normal BN (n = 5)
b. Normal DA (n = 5)
c. isograft (n = 4)
d. allograft (n = 6)

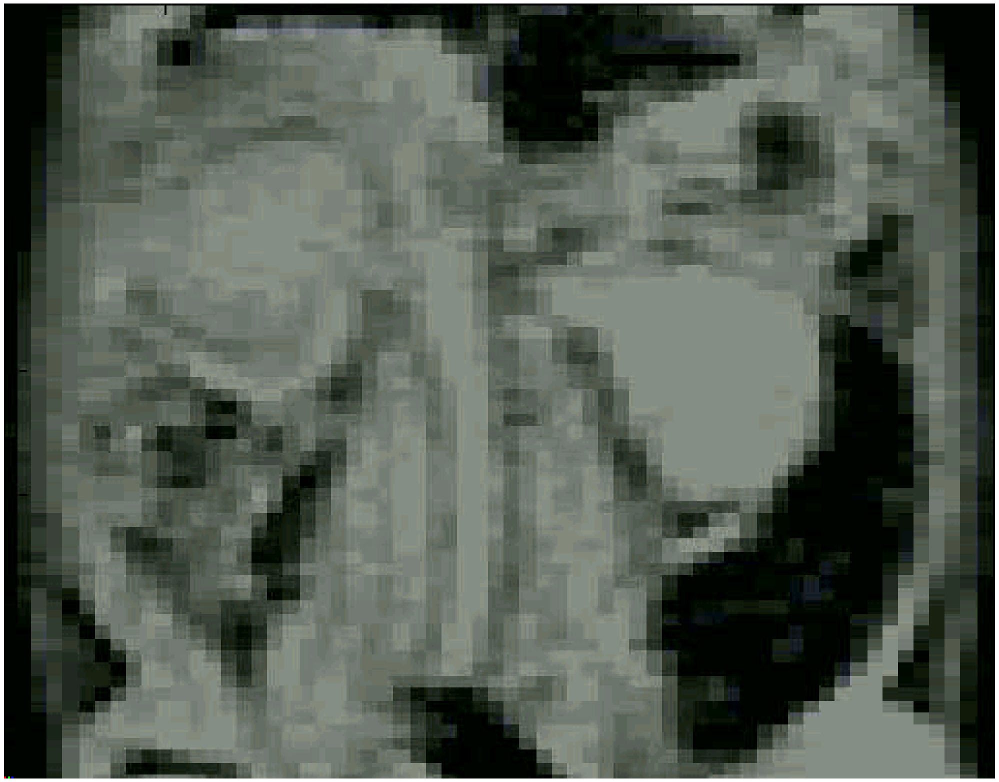

Image size: 64×64
Frame number: 128
Imaging time: 43 Sec

Perfusion Signal: Organ Segmentation

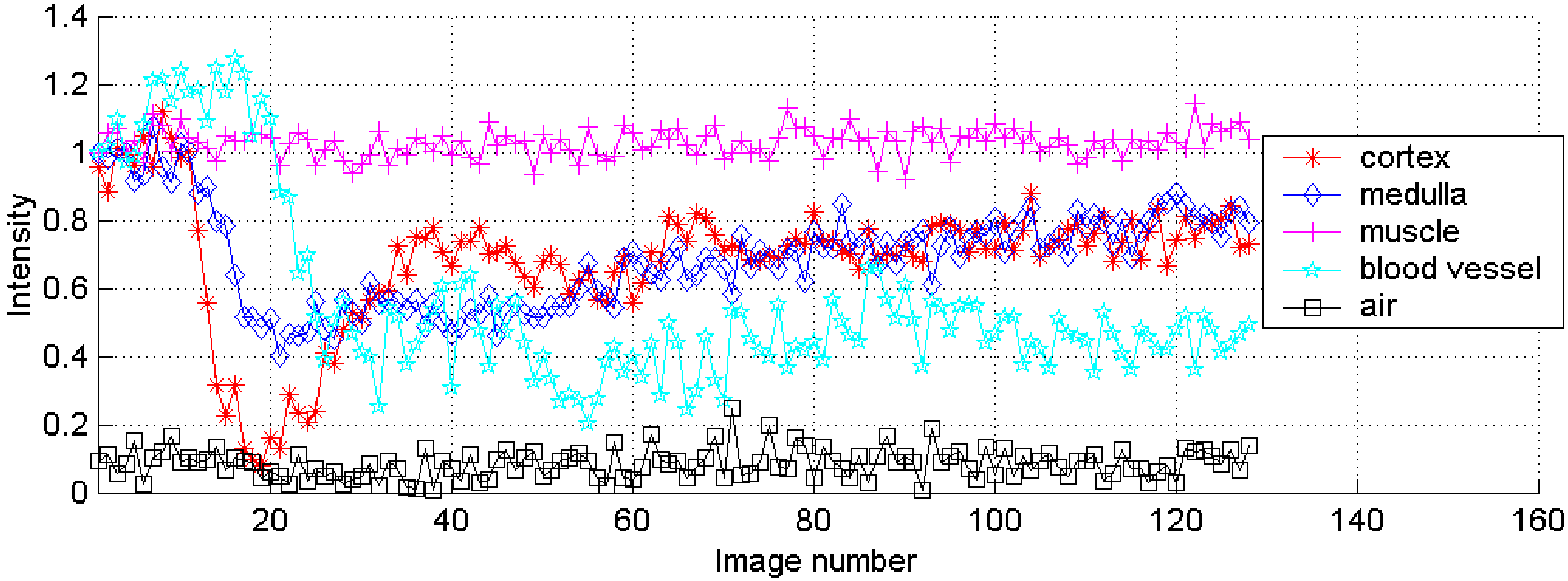

Observation: distinct dynamic features

Perfusion Signal: Function Monitoring

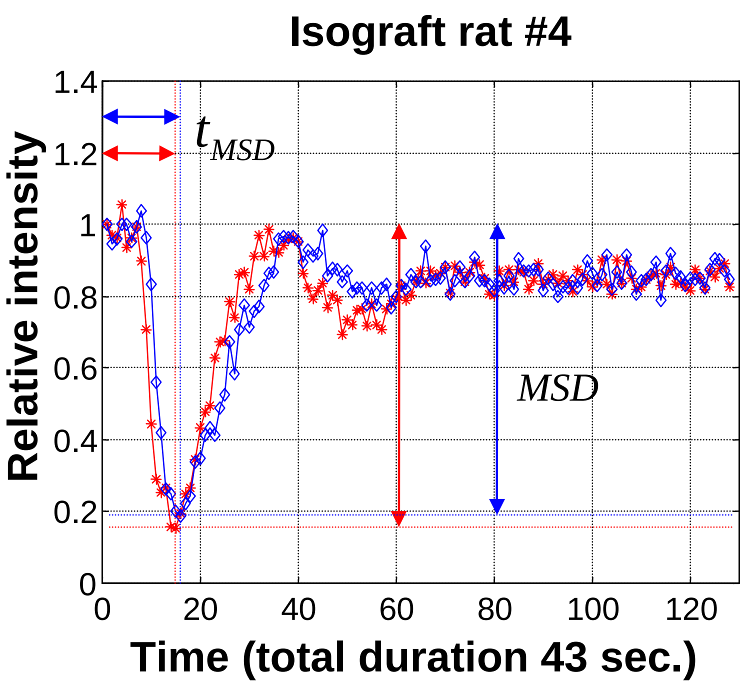

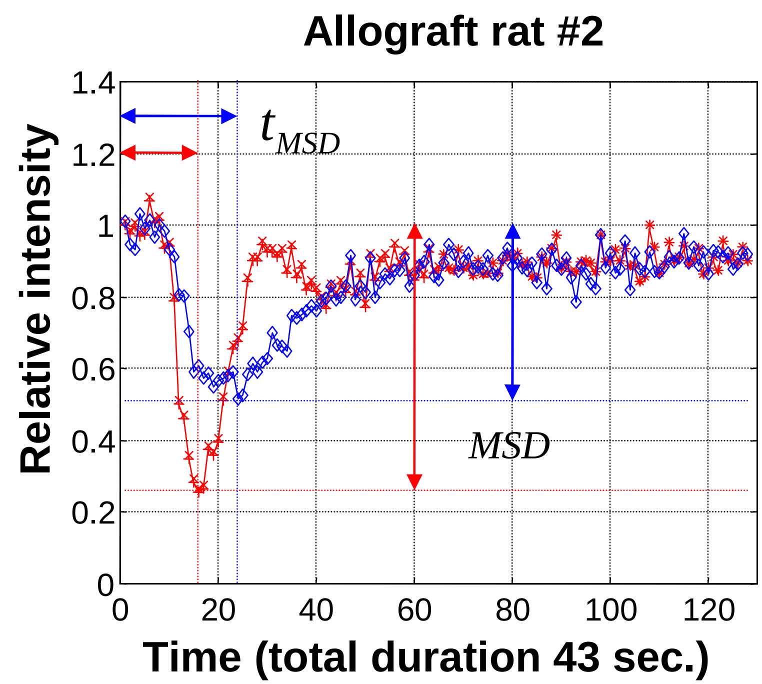

Right (native)
Left (transplanted)

- **MSD: Maximum Signal Decrease**
- **t_{MSD} : Time of occurrence of MSD**
- **Wash-in slope**

Segmentation Algorithm

Preprocessing: Enhance the kidneys and identify their locations

Normal rats: no transplantation

Rats with transplanted kidneys

Energy minimization by level set

Identify the boundary of the cortex

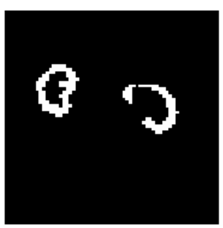

Energy minimization by region-growing

Identify the cortex pixels

Preprocessing

- Mean: $\bar{I}(x,y) = \frac{1}{L}\sum_{t=1}^{L} I(x,y,t)$
- Zero mean signal: $\tilde{I}(x,y,t) = I(x,y,t) - \bar{I}(x,y)$
- Average correlation coefficient

$$\bar{C}(x,y) = (1/8) \sum_{(p,q)\in A(x,y)} \frac{\sum_{t=1}^{L} \tilde{I}(x,y,t)\tilde{I}(p,q,t)}{\sqrt{\sum_{t=1}^{L} \tilde{I}(x,y,t)^2}\sqrt{\sum_{t=1}^{L} \tilde{I}(p,q,t)^2}}$$

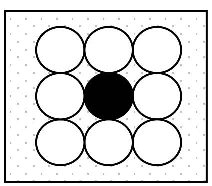

Second order neighborhood structure

$$\begin{aligned} A(x,y) = \{&(x,y-1),(x,y+1),\\ &(x+1,y-1),(x+1,y),\\ &(x+1,y+1),(x-1,y-1),\\ &(x-1,y),(x-1,y+1)\} \end{aligned}$$

MRI sequence

$\Downarrow$

Single image

Locate the Kidneys

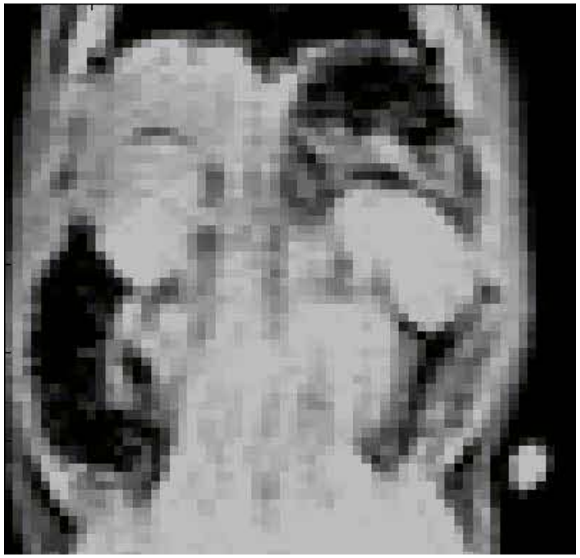

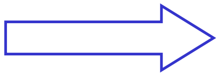

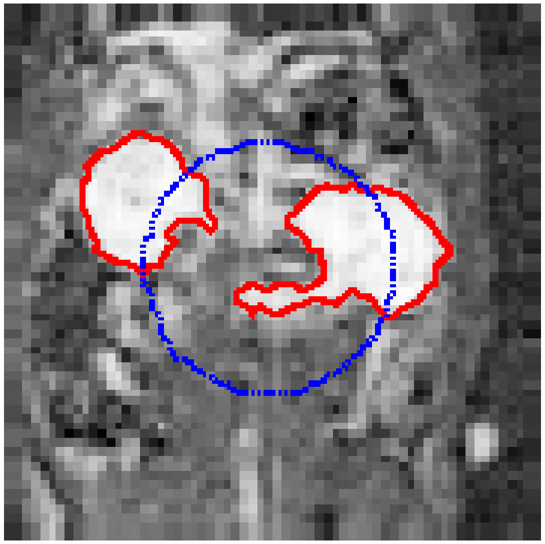

MRI sequence

Single image: $\bar{C}(x, y)$

Kidneys are roughly located: Energy minimization by level set

Normal rats: Cortex segmentation

Energy minimization by level set

C: boundary of a set

Ω_i : inside of curve C

Ω_o : outside of curve C

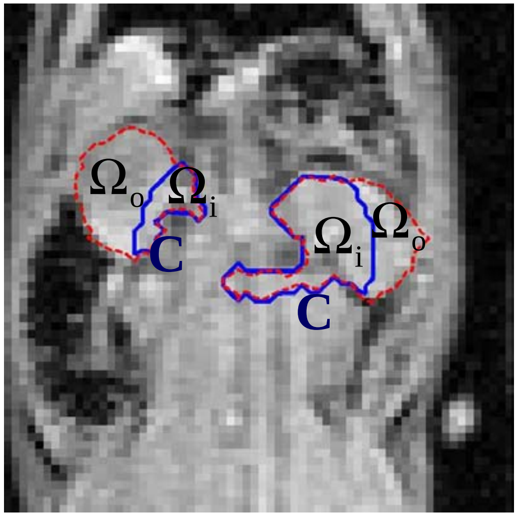

Vector representation

$$\tilde{\mathbf{I}}(x,y)=\left[\tilde{I}(x,y,1),\tilde{I}(x,y,2),\ldots\tilde{I}(x,y,L)\right]$$

$\bar{\mathbf{I}}_i$: average zero mean vector inside curve C

$\bar{\mathbf{I}}_o$: average zero mean vector outside curve C

Energy Minimization: Cortex

- Energy functional

$$E(C) = \mu \cdot \mathrm{Length}(C) + \lambda_1 \int_{\Omega_i} \mathrm{dis}^2\left(\tilde{\mathbf{I}}(x,y), \bar{\mathbf{I}}_i\right) dxdy + \lambda_2 \int_{\Omega_o} \mathrm{dis}^2\left(\tilde{\mathbf{I}}(x,y), \bar{\mathbf{I}}_o\right) dxdy$$

Integral over space

Integral over time sequence

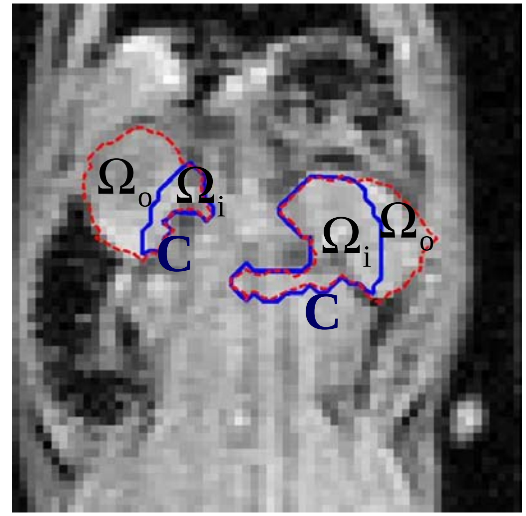

$$\mathrm{dis}^2(\tilde{\mathbf{I}}(x_1,y_1), \tilde{\mathbf{I}}(x_2,y_2)) = \sin^2\frac{\theta}{2} = \frac{1-\cos\theta}{2}$$

$$\cos\theta = \frac{\sum_{t=1}^{L} \tilde{I}(x_1,y_1,t)\tilde{I}(x_2,y_2,t)}{\sqrt{\sum_{t=1}^{L} \tilde{I}(x_1,y_1,t)^2}\sqrt{\sum_{t=1}^{L} \tilde{I}(x_2,y_2,t)^2}}$$

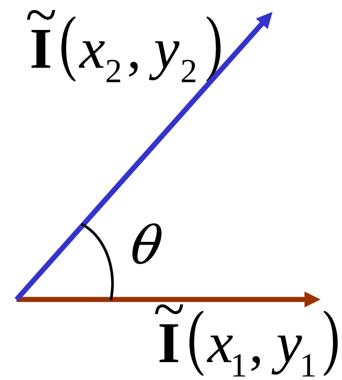

Level set method to minimize energy functional

Transplanted Kidneys

Energy minimization by region growing

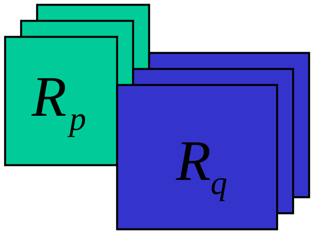

R_p: pth region; N_{Reg}: total number of regions

N_p: total number of pixels in pth region

$\bar{I}^p(t) = \frac{1}{N_p} \sum_{(x,y)\in R_p} I(x,y,t)$; $\bar{\mathbf{I}}^p = [\bar{I}^p(1), \bar{I}^p(2), \cdots, \bar{I}^p(L)]$: average signal

$c(p,q)$: correlation coefficient between two neighboring regions

$$= c(\bar{\mathbf{I}}^p, \bar{\mathbf{I}}^q) = \frac{\sum_{t=1}^{L}\left[\bar{I}^p(t) - \frac{1}{L}\sum_{t=1}^{L}\bar{I}^p(t)\right]\left[\bar{I}^q(t) - \frac{1}{L}\sum_{t=1}^{L}\bar{I}^q(t)\right]}{\sqrt{\sum_{t=1}^{L}\left[\bar{I}^p(t) - \frac{1}{L}\sum_{t=1}^{L}\bar{I}^p(t)\right]^2}\sqrt{\sum_{t=1}^{L}\left[\bar{I}^q(t) - \frac{1}{L}\sum_{t=1}^{L}\bar{I}^q(t)\right]^2}}$$

α: threshold to stop merging

Region-growing

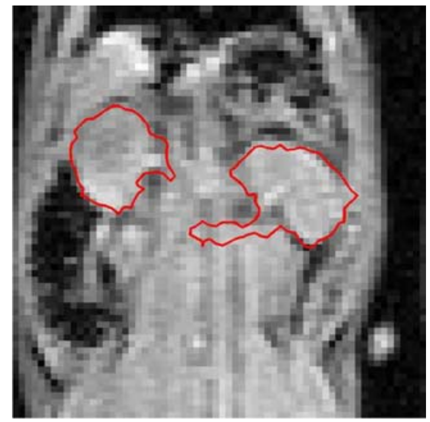

1. For each region, find the average perfusion signal $\bar{\mathbf{I}}^{p}$, $p = 1,2,\ldots,N_{\mathrm{Re}g}$

2. For each pair of neighboring regions, calculate $c(p,q)$ between $\bar{\mathbf{I}}^{p}$ and $\bar{\mathbf{I}}^{q}$

3. Merge R_{p^*} with R_{q^*} s.t. (p^*, q^*) maximizes $c(p,q)$

4. Update the average temporal sequence

$$\bar{\mathbf{I}}^{p^*} = \frac{N_p}{N_p + N_q}\bar{\mathbf{I}}^{p} + \frac{N_q}{N_p + N_q}\bar{\mathbf{I}}^{q}$$

5. Continue merging until $\max c(p,q) < \alpha$

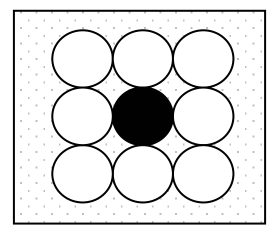

Second order neighborhood structure

Experimental Results

MR instrument: 4.7-T Bruker AVANCE DRX
TR = 3.45ms; TE = 2.1ms
Data matrix size = 64 × 38
USPIO: ultra-small superparamagnetic iron oxide
Dose: 6 mg Fe/kg body weight

Four groups of rats

a. Normal BN (n = 5)
b. Normal DA (n = 5)
c. Isograft BN→BN (n = 4)
d. Allograft DA→BN (n = 6)

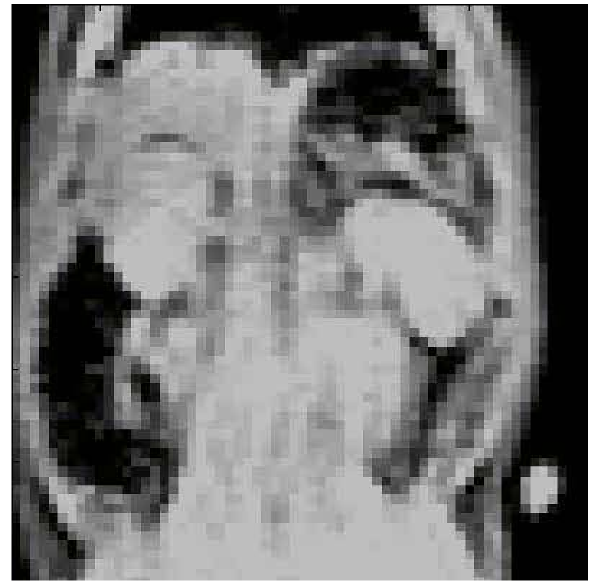

Image size: 64×64
Image number: 128
Imaging time: 43 Sec

Normal rats: No transplantation

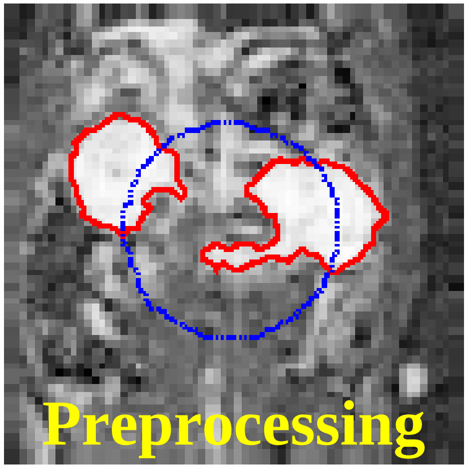

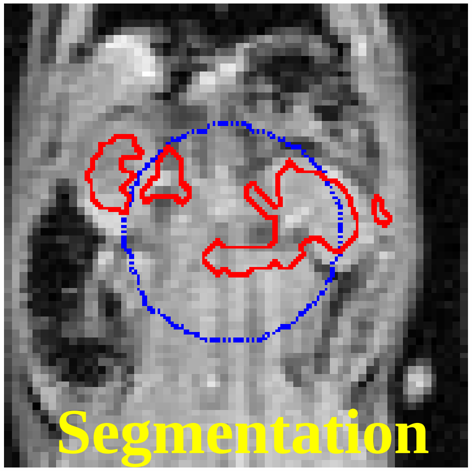

Task1: Automatic Kidney Segmentation

Renal Perfusion Signal

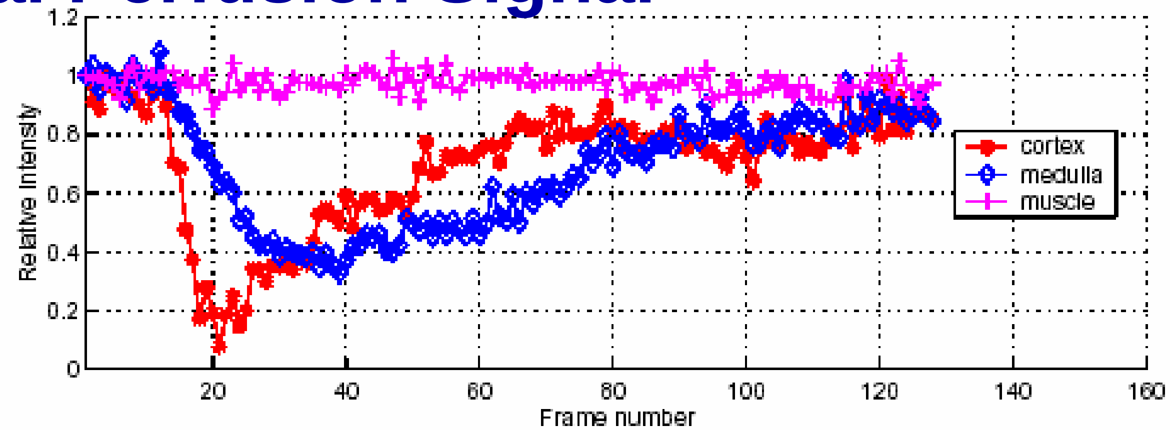

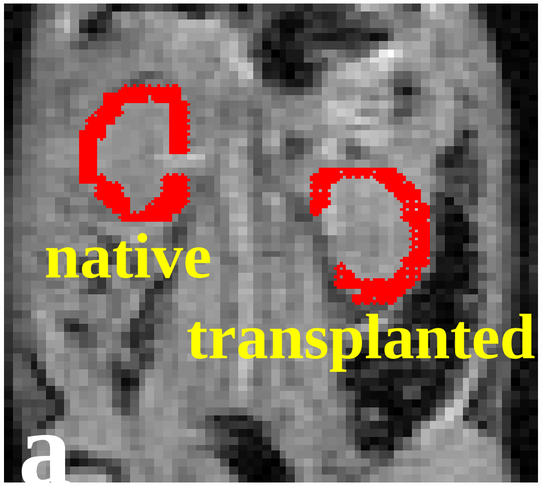

isograft

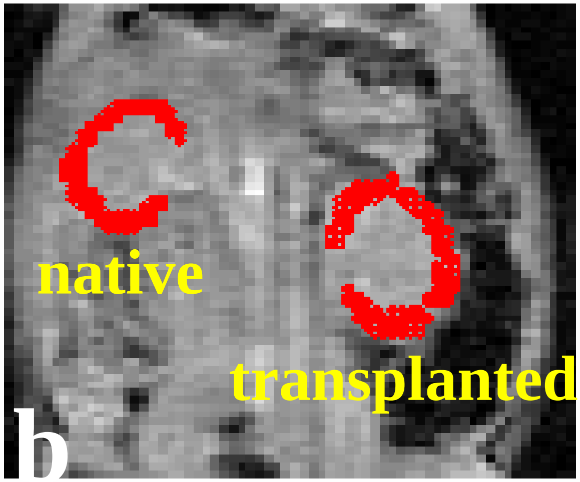

allograft

Task2: Monitoring Organ Function (Kidney)

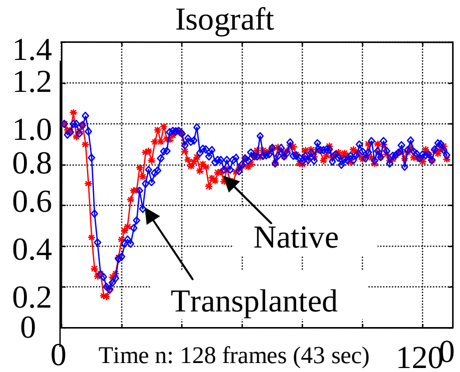

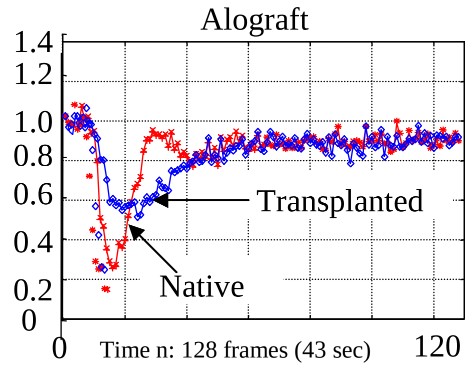

- **Measure of dissimilarity: subspace distance**
  - **Fit a parametric model (AR) to perfusion signal**
  - **Determine (oscillatory) modes of perfusion signal**
  - **Geometric distance between modes of transplanted and native kidneys**

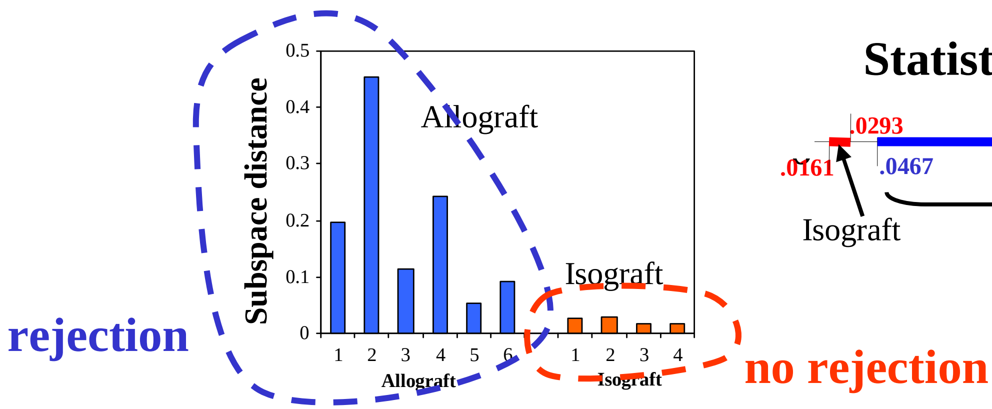

Statistical significance

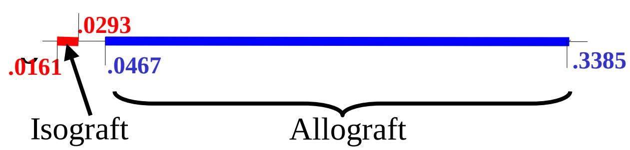

Subspace distance: 6 allograft & 4 isograft rats.

Movement Correction and Noise Reduction

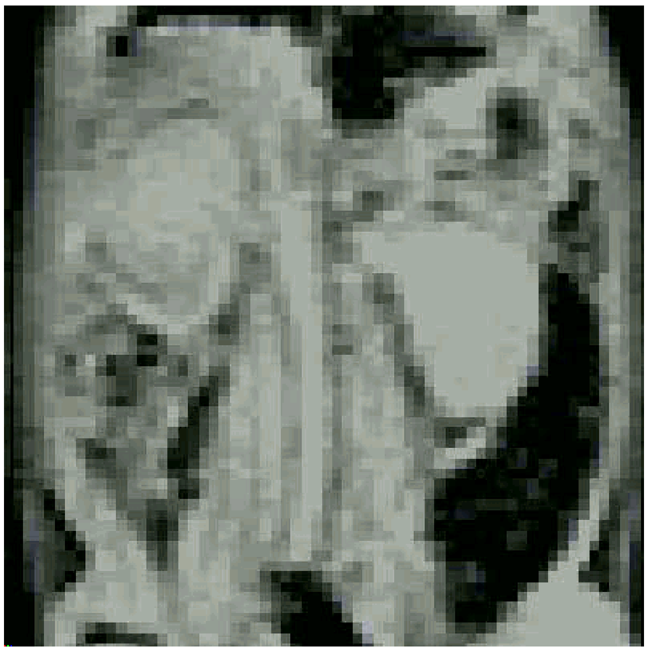

?

Observed

Motion-free & Noiseless

Problem Formulation

Given the observed image sequence $g(i, j, t)$, find the image sequence $f(i, j, t)$ that minimizes

$$E = \underbrace{\left\| g - Hf \right\|^2}_{\text{Motion correction}} + \underbrace{\alpha \left\| \nabla_t f \right\|_W^2 + \beta \left\| \nabla_{tt} f \right\|_W^2}_{\text{Weighted temporal smoothness constraints}}$$

Assume the variance of the background noise is σ^2

$$w(i, j, t) = \exp(1/2)\exp\left(-\frac{p(i, j, t)}{2\sigma^2} \right)$$

Selectively Smooth

$$p(i, j, t) = \frac{1}{2m+1} \sum_{k=-m}^{m} \left(g(i, j, t+k) - \bar{g}(i, j, t) \right)^2 \qquad \bar{g}(i, j, t) = \frac{1}{2m+1} \sum_{k=-m}^{m} g(i, j, t+k)$$

Motion Model

Assumptions:

1. Breathing motion is vertical (head-to-feet) within 1 pixel
2. Motion of pixels along the same horizontal line are identical

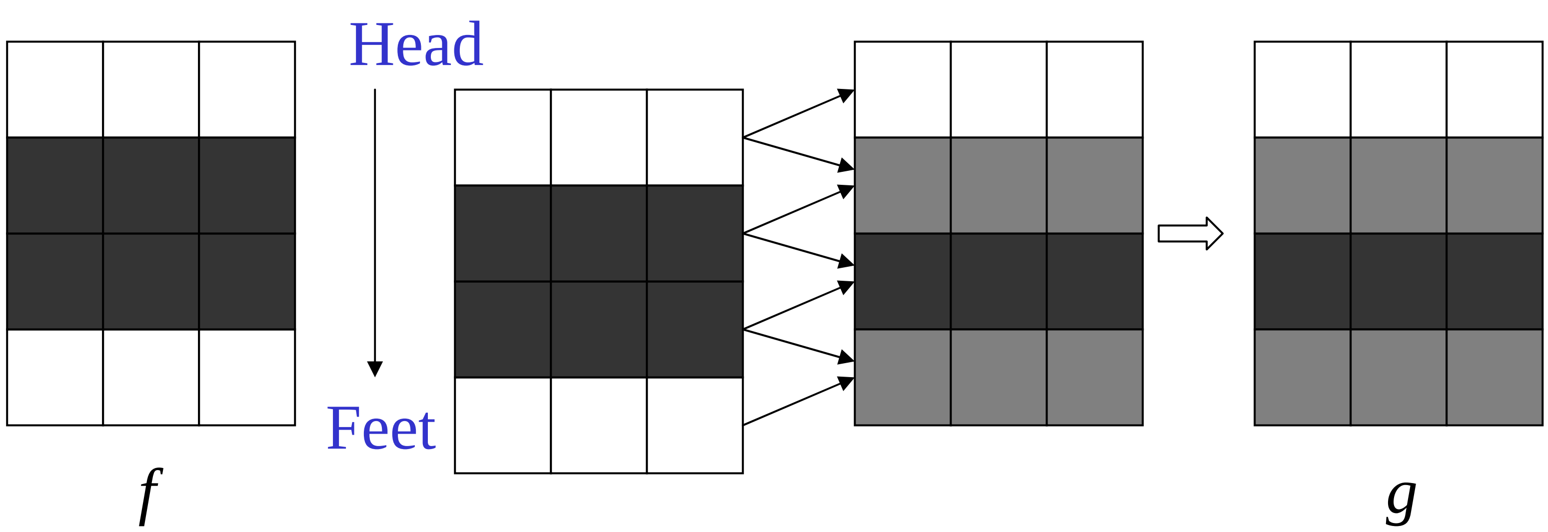

Motion Model (cont'd)

Model non-rigidity:

$$\forall j, \quad g(i,j,t) = \frac{1+d_t}{2}\lambda_{it} f(i-1,j,t) + (1-\lambda_{it}) f(i,j,t) + \frac{1-d_t}{2}\lambda_{it} f(i+1,j,t) + n(i,j,t)$$

$$\begin{cases} d_t = +1, & \text{head} \rightarrow \text{feet} \\ d_t = -1, & \text{head} \leftarrow \text{feet} \end{cases}$$

$$\lambda_{it} = r^{(i-1)}\lambda_t, \quad 0 \le \lambda_t \le 1$$

$$r = 0.95$$

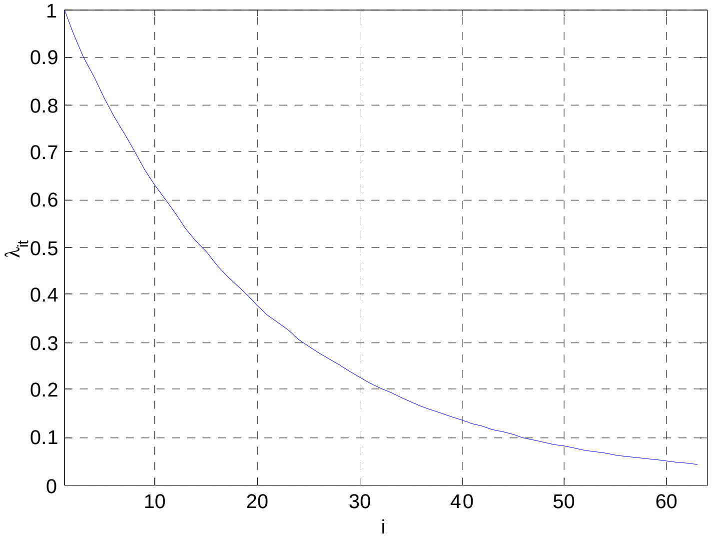

Energy Minimization: matrix-vector form

$$E = (\mathbf{g} - \mathbf{Hf})^{\mathrm{T}} \boldsymbol{\Sigma}^{-1} (\mathbf{g} - \mathbf{Hf}) + \alpha (\mathbf{D}_1 \mathbf{f})^{\mathrm{T}} \mathbf{W} (\mathbf{D}_1 \mathbf{f}) + \beta (\mathbf{D}_2 \mathbf{f})^{\mathrm{T}} \mathbf{W} (\mathbf{D}_2 \mathbf{f})$$

Keeping **H** fixed,

$$\mathbf{f}^* = \left[\mathbf{H}^{\mathrm{T}} \boldsymbol{\Sigma}^{-1} \mathbf{H} + \alpha \left(\mathbf{D}_1{}^{\mathrm{T}} \mathbf{W} \mathbf{D} \right)_1 + \beta \left(\mathbf{D}_2{}^{\mathrm{T}} \mathbf{W} \mathbf{D} \right)_2 \right]^{-1} \mathbf{H}^{\mathrm{T}} \boldsymbol{\Sigma}^{-1} \mathbf{g}$$

$\Downarrow$ Avoid inversion of a $(N_i \times N_j \times N_t)^2$ matrix

Minimize two energy functions iteratively

$$E_1 = (\tilde{\mathbf{g}} - \mathbf{f})^{\mathrm{T}} \boldsymbol{\Sigma}^{-1} (\tilde{\mathbf{g}} - \mathbf{f}) + \alpha (\mathbf{D}_1 \mathbf{f})^{\mathrm{T}} \mathbf{W} (\mathbf{D}_1 \mathbf{f}) + \beta (\mathbf{D}_2 \mathbf{f})^{\mathrm{T}} \mathbf{W} (\mathbf{D}_2 \mathbf{f})$$

$$E_2 = (\mathbf{g} - \mathbf{Hf})^{\mathrm{T}} \boldsymbol{\Sigma}^{-1} (\mathbf{g} - \mathbf{Hf}), \quad \tilde{\mathbf{g}} = \mathbf{H}^{\mathrm{T}} \mathbf{g}$$

Results

$\alpha = 1, \quad \beta = 2$

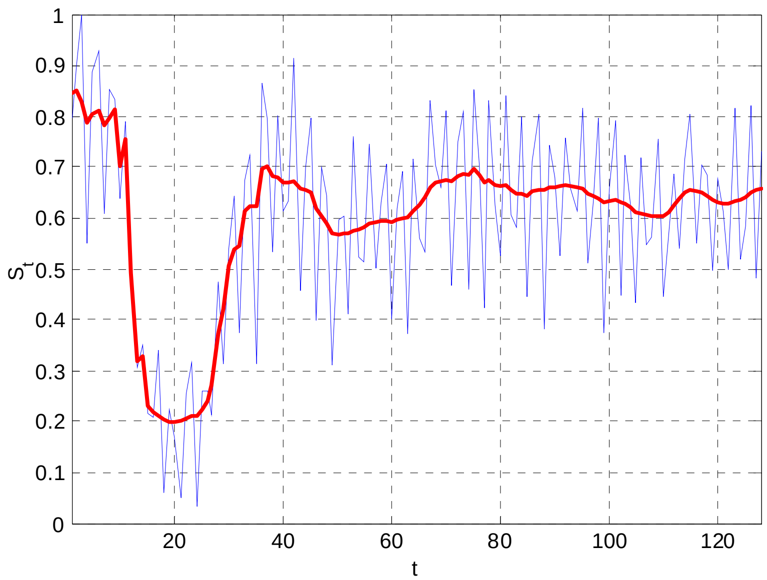

Original and recovered signals

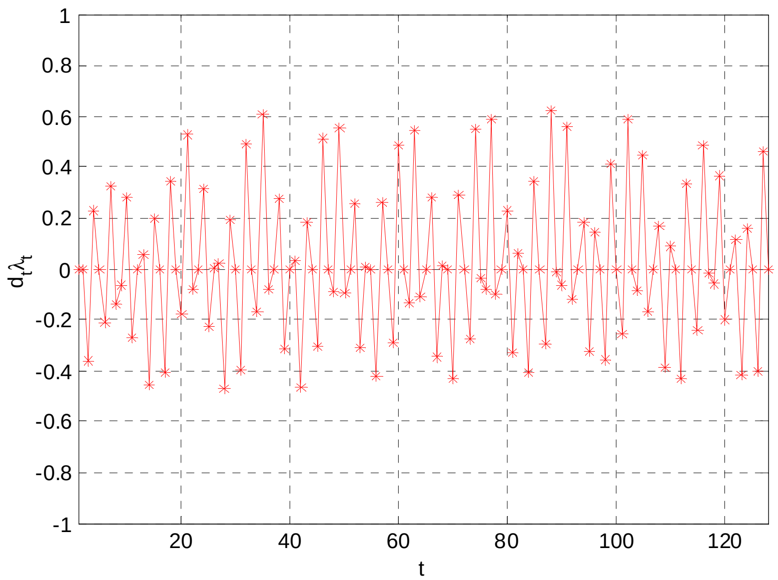

Movement

Results (isograft)

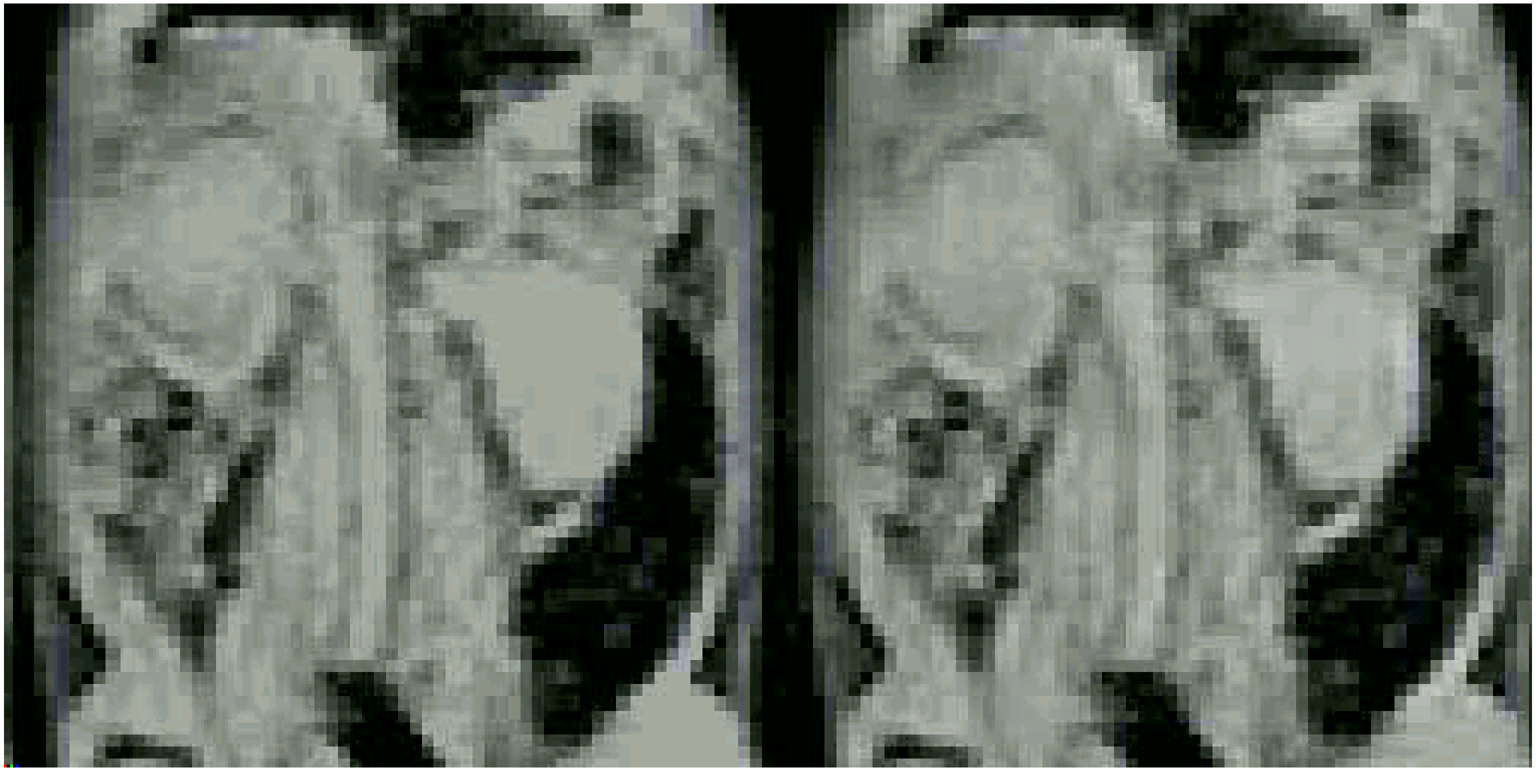

Observed (*g*) Recovered (*f*)

Results (allograft)

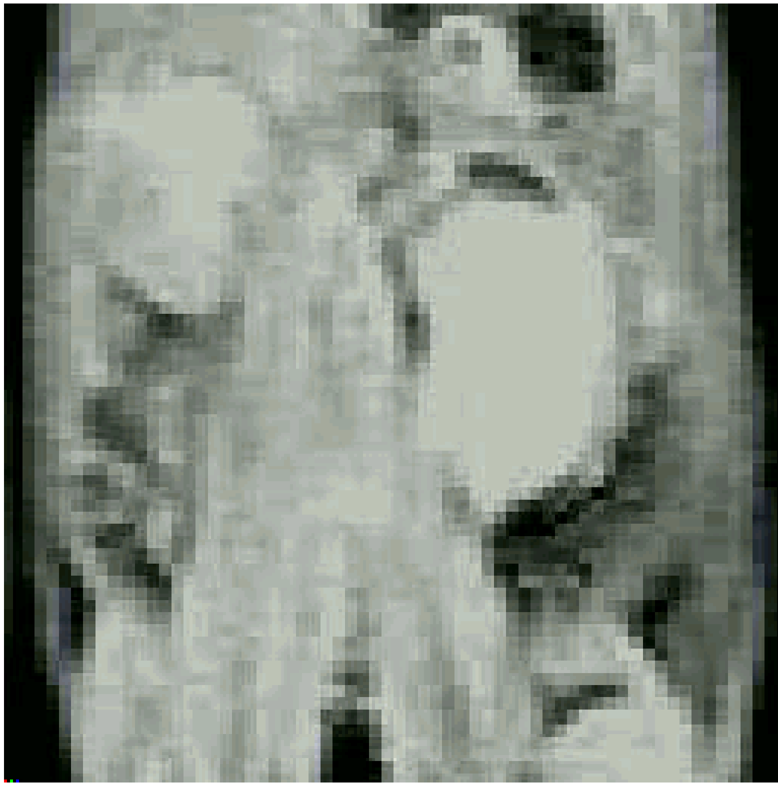

Observed (g)

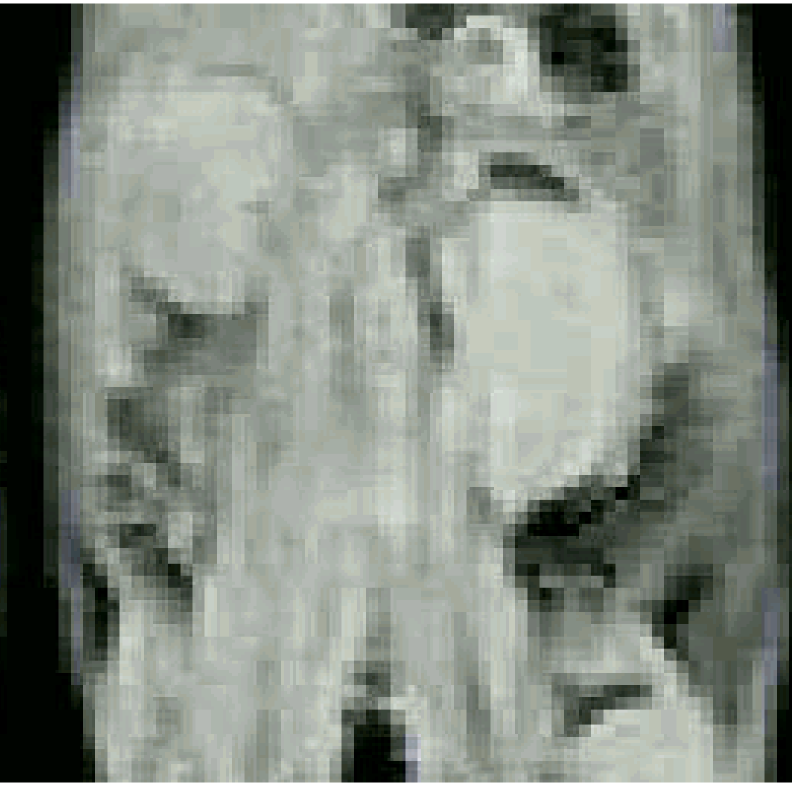

Recovered (f)

Heart

- **Heart segmentation**
- **Heart structures segmentation**
- **Motion tracking**
- **Data:**
  - **Untagged**
  - **Tagged**

Untagged Data: Active Contour Methods

- Kass, Witkin & Terzopoulos: classical snakes, edge-based
- Cohen: balloon snake, edge-based + constant force
- Xu & Prince: snake edge-based +new potential force field, Gradient Vector Field, (GVF)
- Malladi, Sethian & Vemuri method: edge-based + constant force
- Chan & Vese method: region-based + piecewise constant model

Problems with existing methods

- Edge-based: only local information, sensitive to initial condition
- Initial contour must reside close enough to true boundary of the object, or contour will not move if no edge information is present, contour may be trapped at spurious edge points
- Adding an external constant force causes leakage where edge of the object boundary is weaker than added constant force
- Piece-wise constant model fails when the image has low contrast

Automatic Heart Segmentation: Results Current Methods

Gradient Vector Field (Xu & Prince)

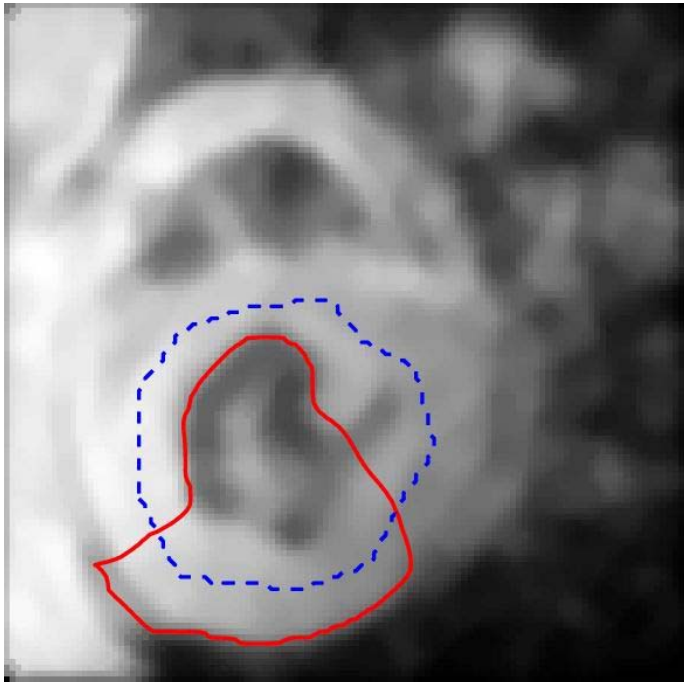

Chan & Vese Energy Minimization

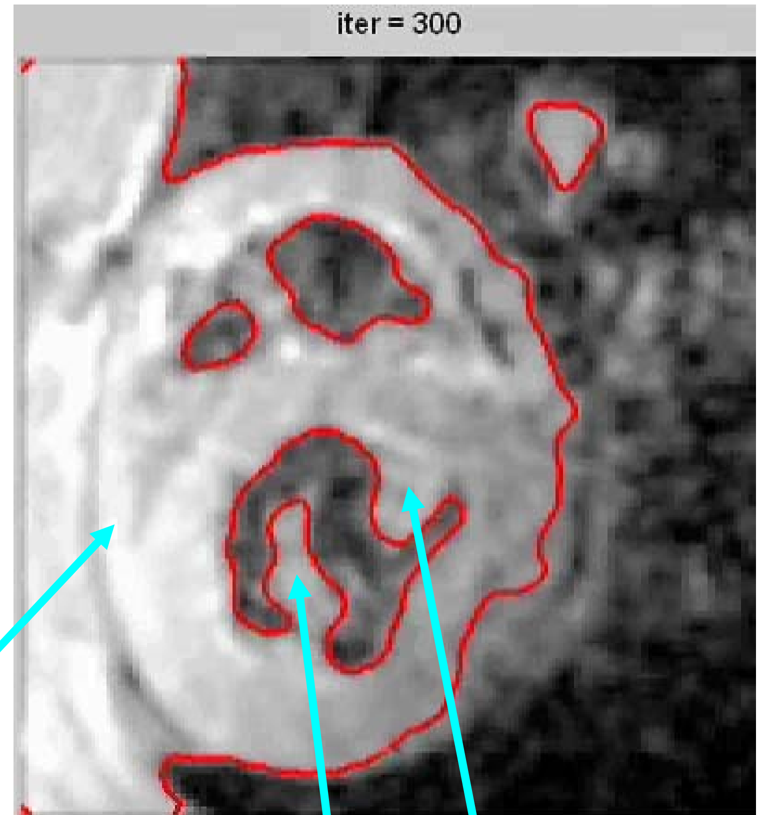

Initial contour not close enough to desired left ventricular endocardium, contour converges to undesired boundary

Chest wall not segmented

Papillary muscles not segmented

Problems: low contrast, lack edge information, no prior on shape

Energy Minimization: Stochastic Active Contour

- **Stochastic model: Works with low contrast, segments chest wall**
- **Region-based + Edge-based: robust to contour's initial condition**
- **Prior knowledge about shape of heart: papillary muscle problem**

$$J(C) = \lambda_1 J_1(C) + \lambda_2 J_2(C) + \lambda_3 J_3(C) + \lambda_4 J_4(C)$$

Model Matching (e.g., temporal)

Image gradient (Texture)

Prior Knowledge (Shape)

Contour Smoothing (Snake)

Minimization solution: PDE contour evolution & level sets

- **Provides smooth and closed boundary**
- **Deformable: segments various anatomy parts**
- **High potential for tracking motion of heart**

Region-based forces: Contour not trapped at spurious edge points

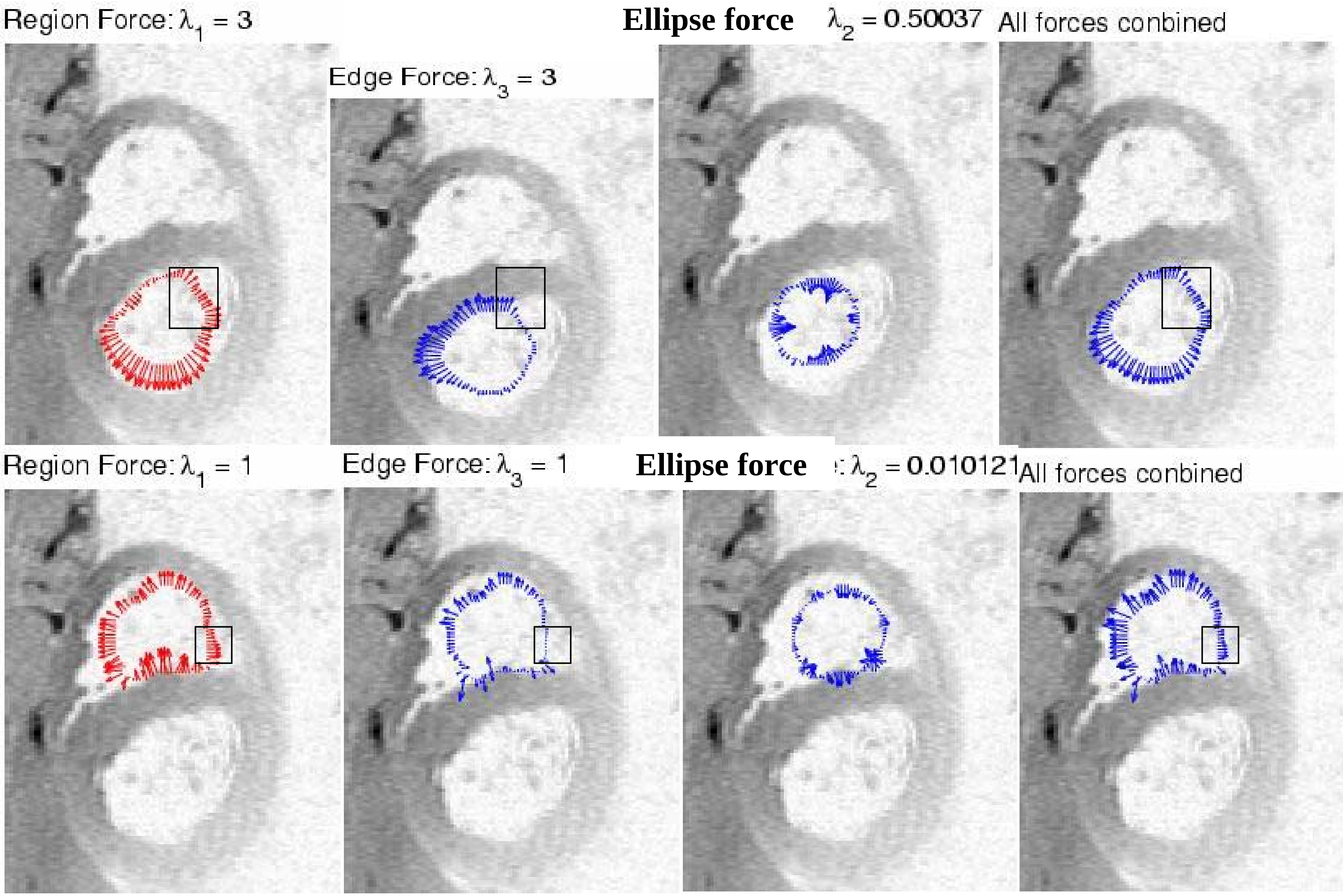

Region-based forces: Contour keeps moving although edge information missing

Region-based forces and edge-based forces: Balance keeps contour stationary at object boundary.

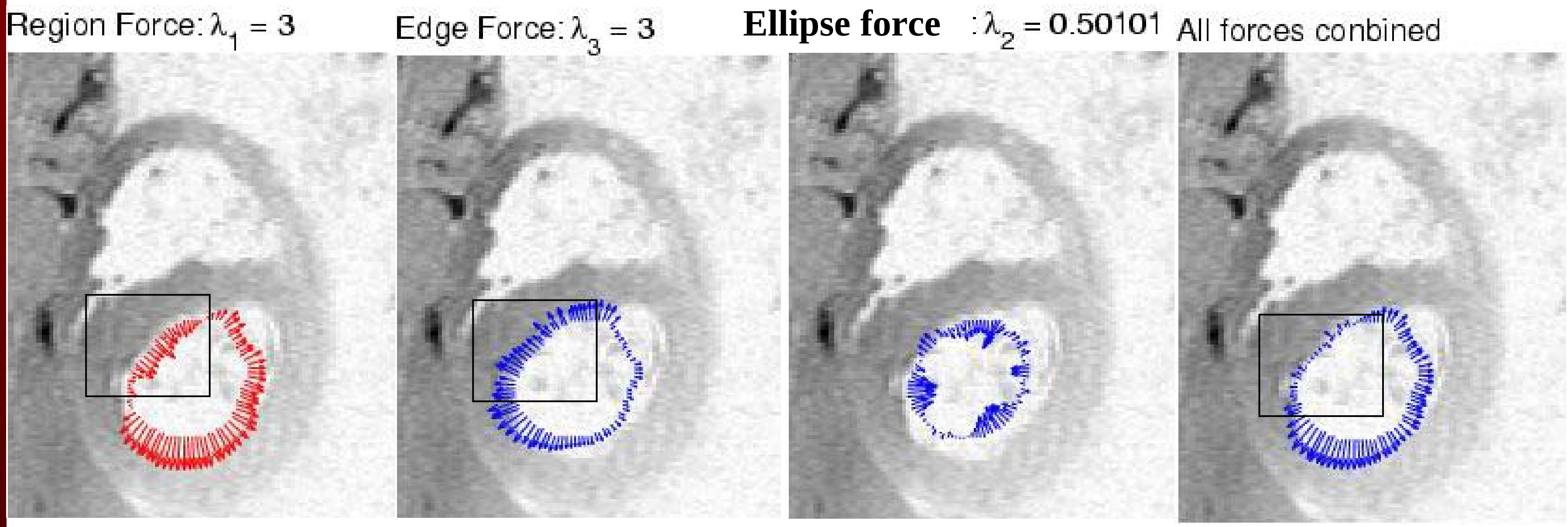

Automatic Heart Segmentation

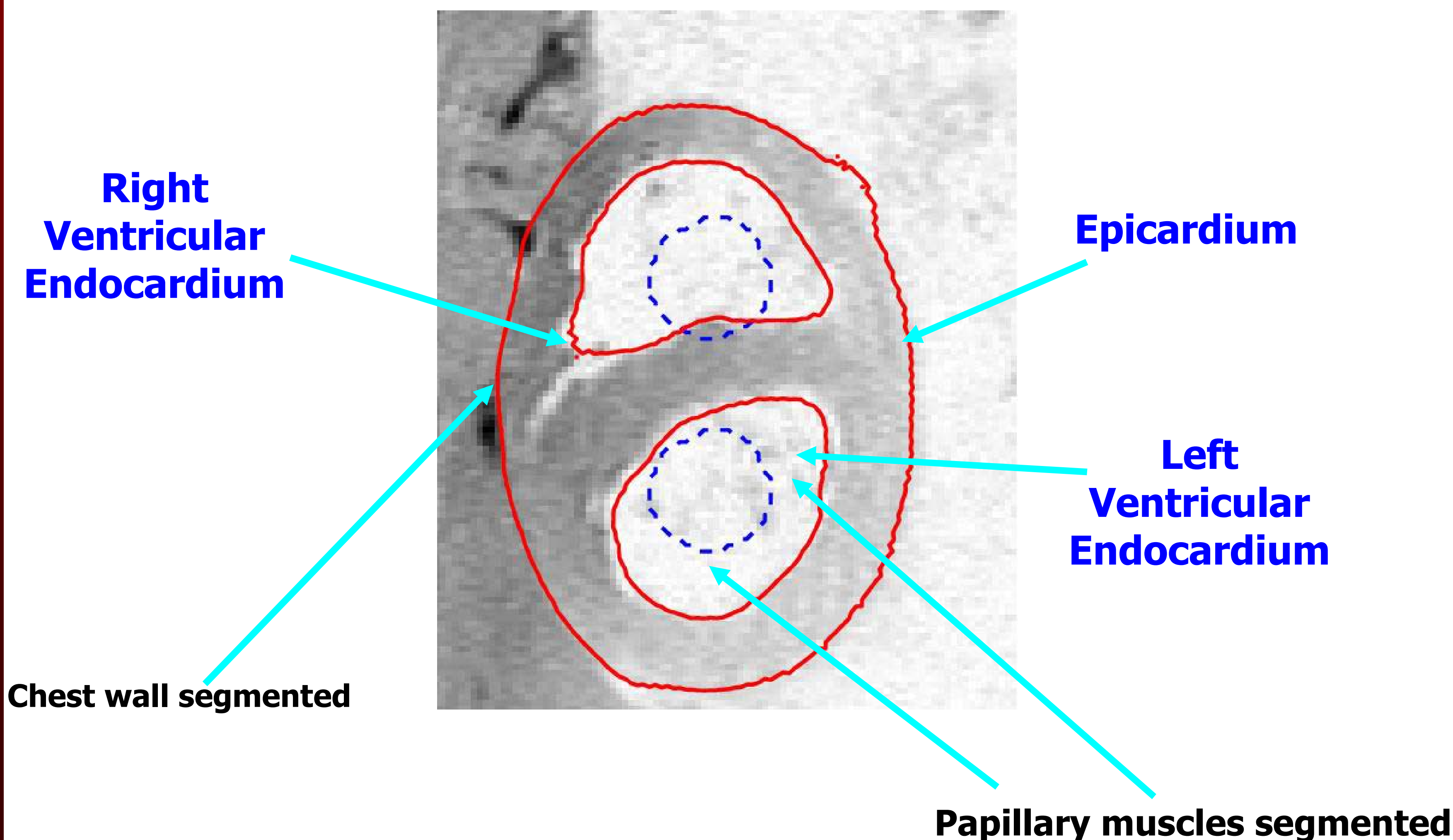

Contours tracked using Stochastic Active Contour Scheme

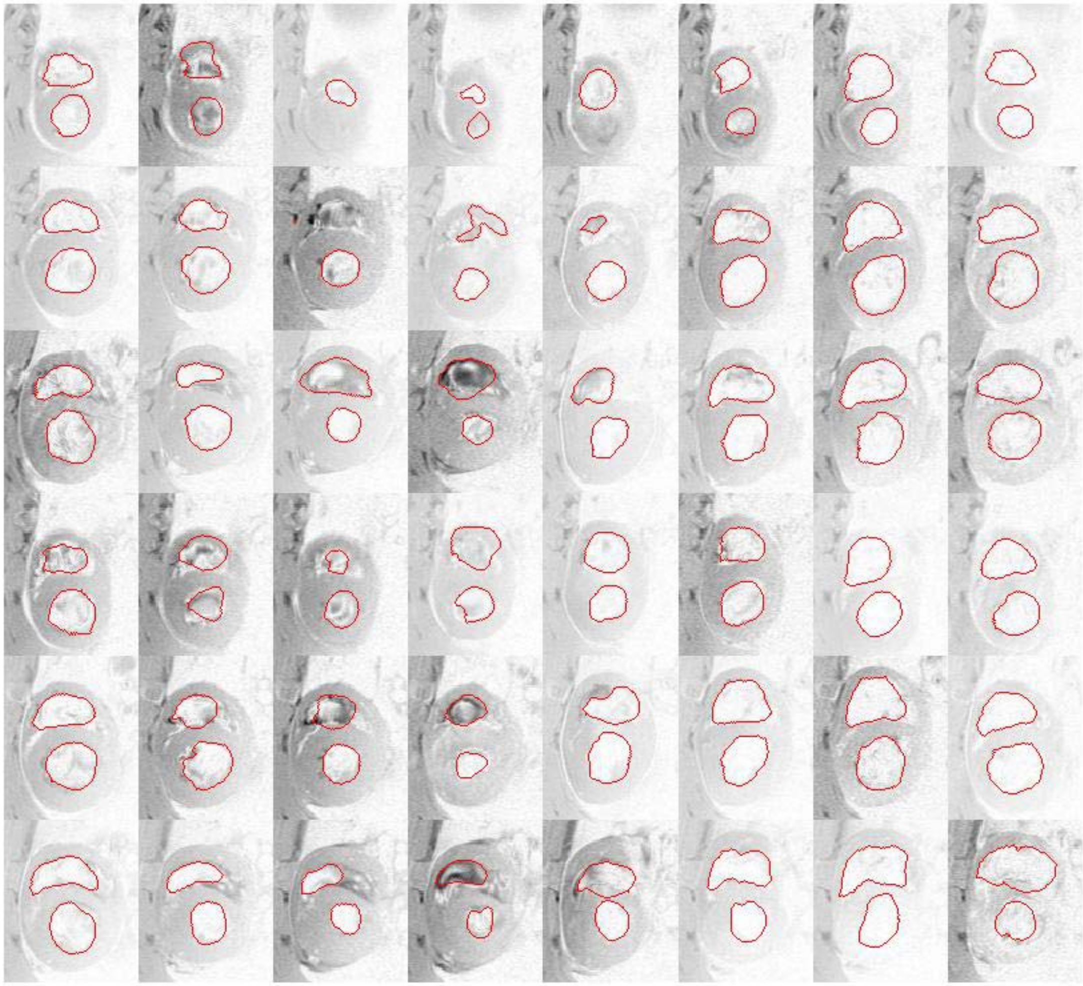

Contours tracked manually

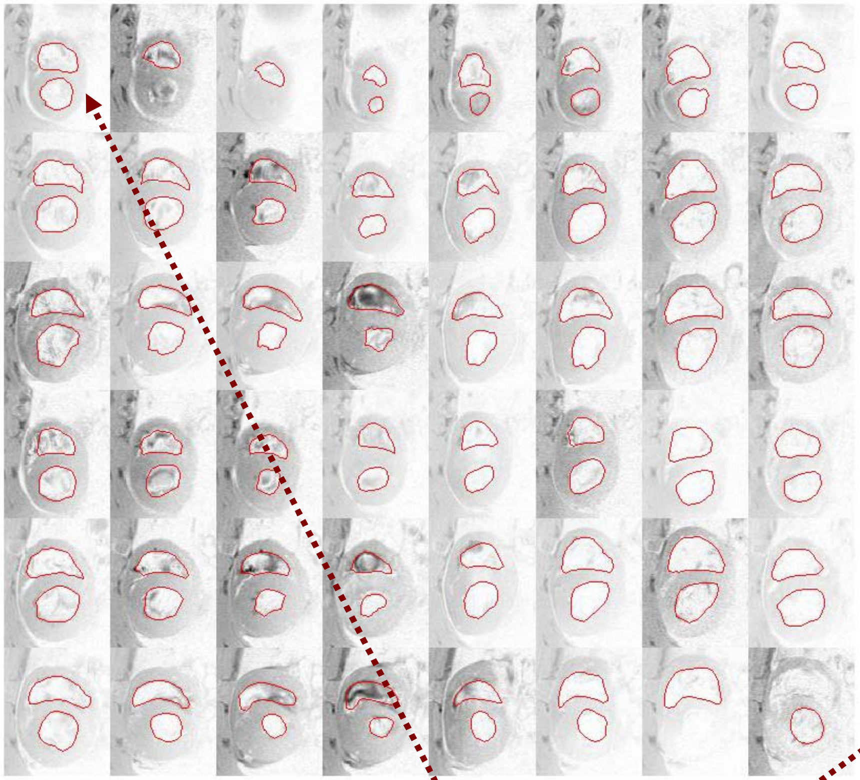

Contours tracked using Stochastic Active Contour Scheme

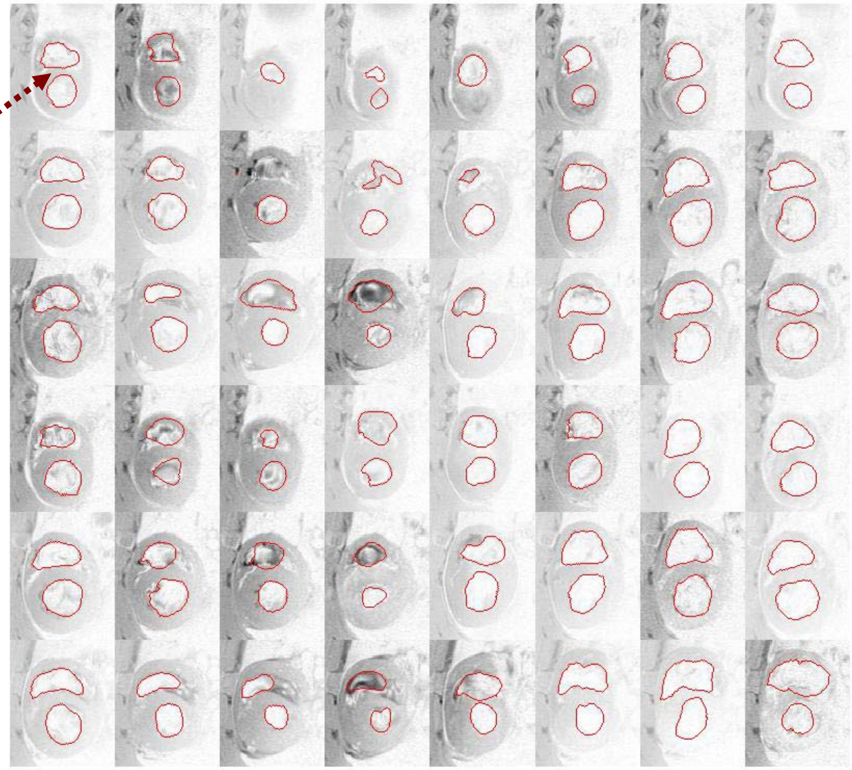

How good is automatic segmentation?

Similarity Between Reference and Segmented Contours

(Modified Chanfer)

$$s(E_r, E_c) = \frac{\sum_{(x,y)} S(x,y) \cdot \Gamma_r(x,y)}{\sum_{(x,y)} S(x,y)}$$

Edge Similarity

$$s(\boldsymbol{A}, \boldsymbol{B}) = \frac{2 * \boldsymbol{n}(\boldsymbol{A} \cap \boldsymbol{B})}{\boldsymbol{n}(\boldsymbol{A}) + \boldsymbol{n}(\boldsymbol{B})}$$

Area Similarity

LV

$$\begin{bmatrix} 0.6519 & 0 & 0 & 0.5103 & 0 & 0.4796 & 0.6371 & 0.586 \\ 0.6286 & 0.6198 & 0.6690 & 0.6994 & 0.6741 & 0.7236 & 0.6070 & 0.518 \\ 0.5225 & 0.6857 & 0.6650 & 0.6529 & 0.6760 & 0.6591 & 0.6520 & 0.614 \\ 0.6618 & 0.4943 & 0.5845 & 0.5804 & 0.5465 & 0.6855 & 0.5878 & 0.578 \\ 0.6570 & 0.5470 & 0.6428 & 0.6831 & 0.6330 & 0.7141 & 0.4918 & 0.640 \\ 0.5826 & 0.6136 & 0.6948 & 0.6282 & 0.7191 & 0.6210 & 0 & 0.423 \end{bmatrix} \quad \begin{bmatrix} 0.9182 & 0 & 0 & 0.6844 & 0 & 0.7075 & 0.8971 & 0.933 \\ 0.9384 & 0.9145 & 0.9212 & 0.9183 & 0.8969 & 0.9632 & 0.9098 & 0.860 \\ 0.8607 & 0.9298 & 0.9391 & 0.8660 & 0.9547 & 0.9149 & 0.9013 & 0.882 \\ 0.9412 & 0.7391 & 0.8451 & 0.7744 & 0.8526 & 0.9358 & 0.8875 & 0.919 \\ 0.9423 & 0.8525 & 0.8541 & 0.9026 & 0.9052 & 0.9534 & 0.8612 & 0.928 \\ 0.8917 & 0.8678 & 0.9418 & 0.8328 & 0.9354 & 0.8462 & 0 & 0.776 \end{bmatrix}$$

$$\begin{bmatrix} 0.6303 & 0.3480 & 0.6519 & 0.6131 & 0.6268 & 0.6047 & 0.6309 & 0.606 \\ 0.6380 & 0.6199 & 0 & 0.2057 & 0.3030 & 0.5901 & 0.6262 & 0.606 \\ 0.6136 & 0.4766 & 0.5757 & 0.5670 & 0.5586 & 0.6771 & 0.6475 & 0.587 \\ 0.5925 & 0.3239 & 0.5202 & 0.3228 & 0.5477 & 0.6806 & 0.5583 & 0.636 \\ 0.6550 & 0.5713 & 0.5142 & 0.6326 & 0.4431 & 0.6500 & 0.5985 & 0.649 \\ 0.5623 & 0.6041 & 0.5644 & 0.5378 & 0.4748 & 0.5754 & 0.6383 & 0 \end{bmatrix} \quad \begin{bmatrix} 0.8395 & 0.6414 & 0.8452 & 0.7297 & 0.8802 & 0.7987 & 0.8974 & 0.826 \\ 0.8927 & 0.8328 & 0 & 0.2820 & 0.3492 & 0.8953 & 0.9070 & 0.902 \\ 0.8598 & 0.6315 & 0.8275 & 0.7955 & 0.7823 & 0.9182 & 0.9235 & 0.860 \\ 0.8134 & 0.6470 & 0.5646 & 0.6691 & 0.8470 & 0.9273 & 0.8357 & 0.907 \\ 0.9056 & 0.7452 & 0.7428 & 0.8185 & 0.7901 & 0.9262 & 0.8693 & 0.900 \\ 0.8172 & 0.8047 & 0.6539 & 0.6988 & 0.7938 & 0.8888 & 0.9282 & 0 \end{bmatrix}$$

RV

Comparison

Contour tracked by our Active Contour scheme

Contour tracked manually

LV

RV

Edge Similarity = 0.7141

Area Similarity = 0.9534

Edge Similarity = 0.6500

Area Similarity = 0.9262

Tagline Detection: tag centers

- Three types of tag centers:
  - Vertical taglines, horizontal taglines, and crossings of both taglines
  - Each type of tag centers is associated with a model

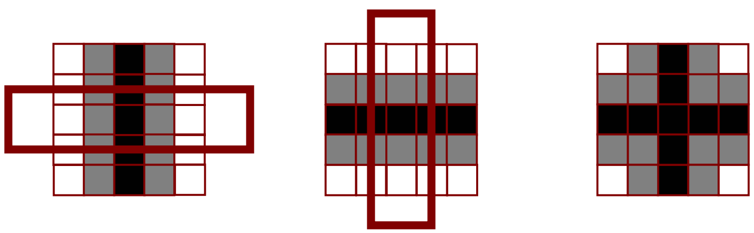

Vertical model **Horizontal model** **Crossing model**

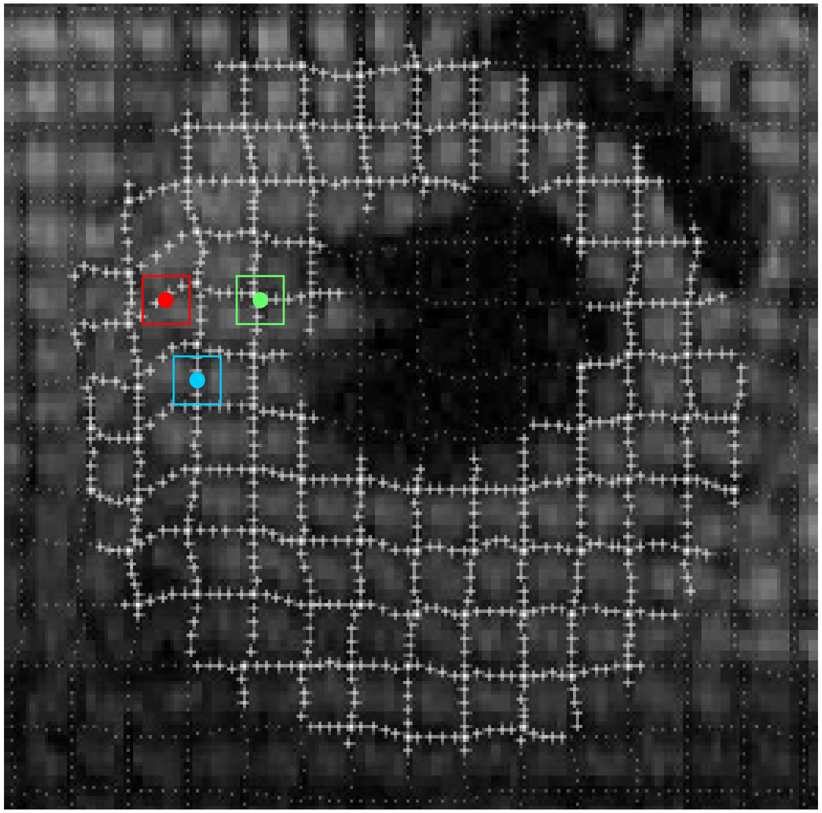

Heart Segmentation

- **Tagged Data**

Key Observations

- Tagline prediction
  - Predict initial tag positions based on motion between two previous frames

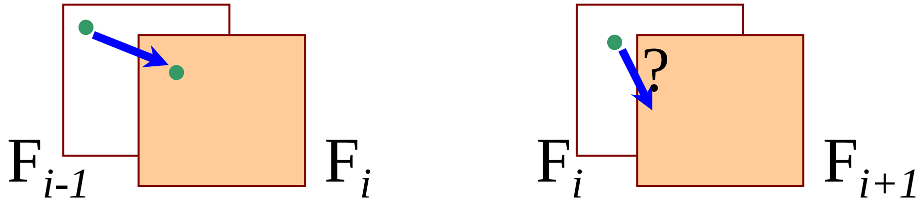

- Motion of the taglines: sparse
  - Model movement and then construct dense displacement field

Tagged Data: Heterotropic Heart Transplantation

Isograft No Rejection

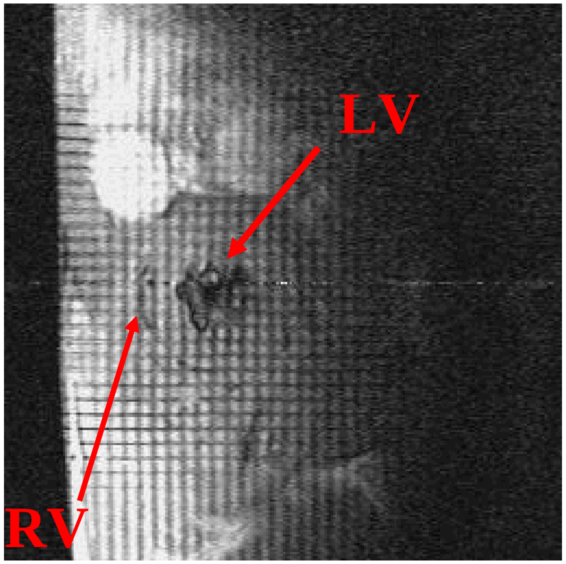

Allograft With Rejection

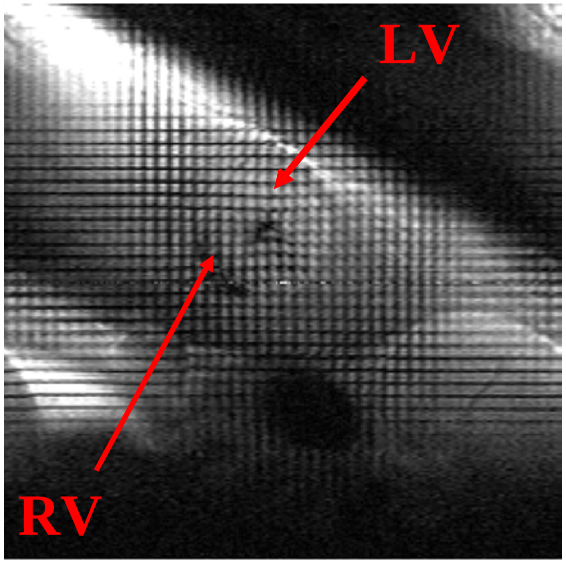

Goal: by monitoring the ***motion*** of every pixel in the heart, monitor the ***function*** of the heart

Challenge: detect motion of every pixel in myocardium

Heart Motion Detection

- **Estimate dense motion of the heart from first detecting motion of taglines**
- **Expand motion of taglines to motion of every myocardial pixel.**
- **Many existing techniques:**
  - **Single tagline detection: nothing to prevent two taglines from occupying same physical position**
  - **Valuable correlations between adjacent taglines are ignored**

Data

- **Transplanted rats with heterotropic working heart.**
- **Cardiac tagging achieved by a modified DANTE sequence.**
- **MRI scans were performed on a Bruker AVANCE DRX 4.7-T system.**
- **8 to 12 frames per cardiac cycle.**
- **The size of each matrix is 256×256 pixels.**

Our Methodology

- Simultaneous detection of all tag lines: Energy minimization

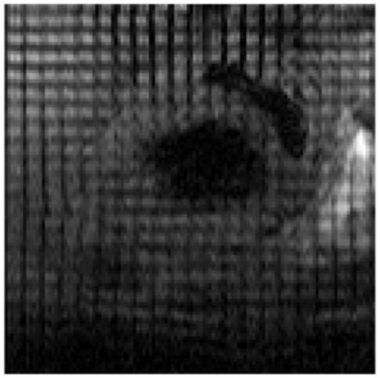

- Taglines motion (displacement) field

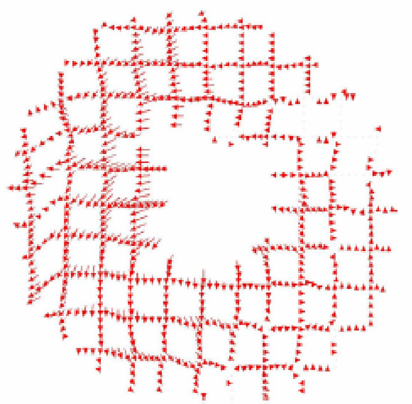

- Motion of myocardial pixels: dense motion field

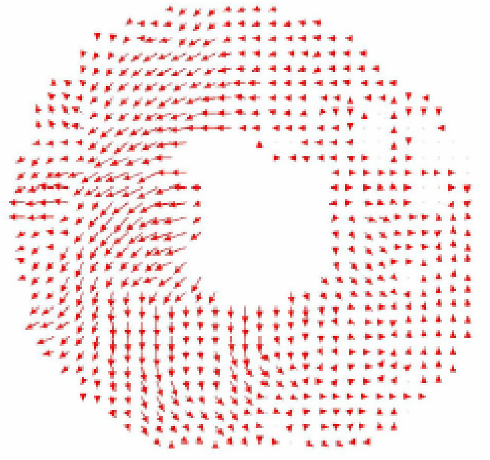

Task2: Tagline Detection

For each frame in cardiac cycle from diastole to systole:

Preprocessing: Get distance maps

⇩

Initialize taglines: Predict motion of taglines

⇩

Deform taglines: Minimize energy functional

⇩

Compute the motion of the taglines

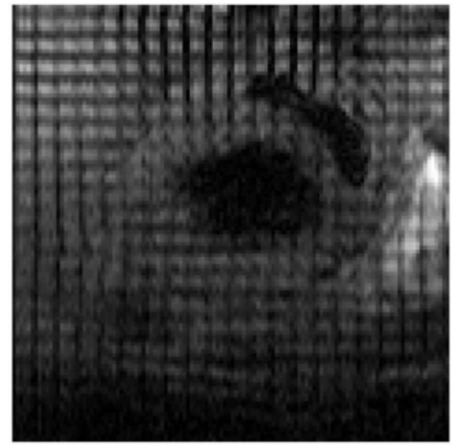

I

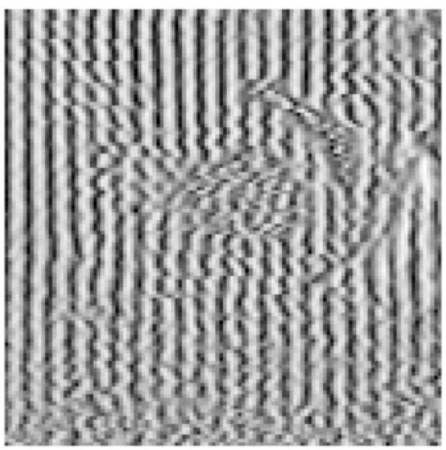

I_V

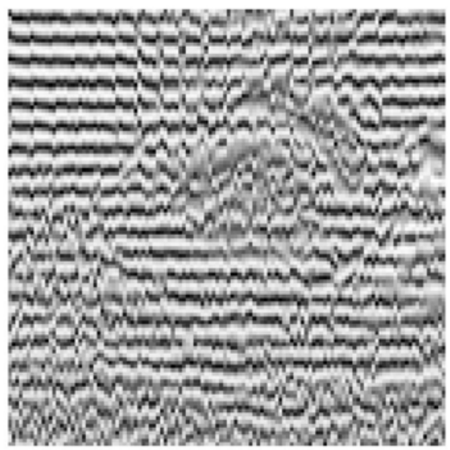

I_H

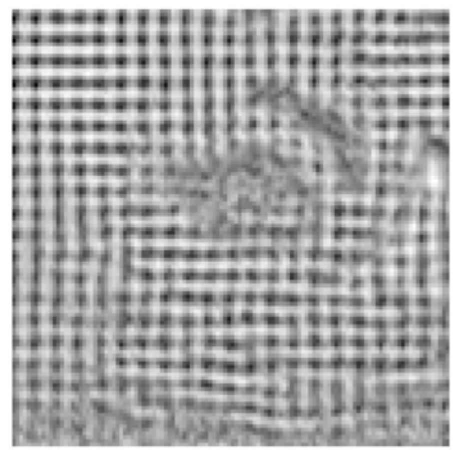

I_C

Tagline Detection: energy functional

For the pixel (*x*,*y*) on a mesh, the energy functional is:

$$\begin{aligned} E\left(\left\{x_{ij}, y_{ij}\right\}\right) = & \sum_{(i,j)\in V} [\alpha_V E_{V\mathrm{int}}(x_{ij}, y_{ij}) + \beta_V D_V(x_{ij}, y_{ij})] + \\ & \sum_{(i,j)\in H} [\alpha_H E_{H\mathrm{int}}(x_{ij}, y_{ij}) + \beta_H D_H(x_{ij}, y_{ij})] + \\ & \sum_{(i,j)\in C} [\alpha_C E_{C\mathrm{int}}(x_{ij}, y_{ij}) + \beta_C D_C(x_{ij}, y_{ij})] \end{aligned}$$

Internal Energy

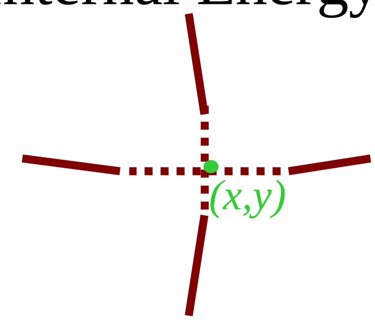

Distance Metrics

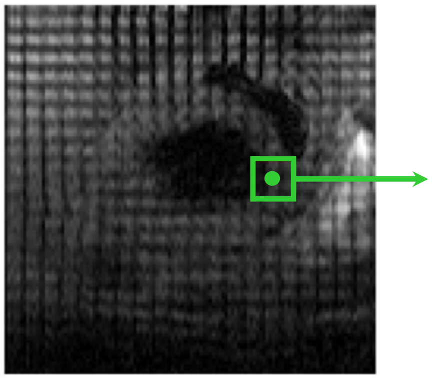

Tagline Detection: distance metrics

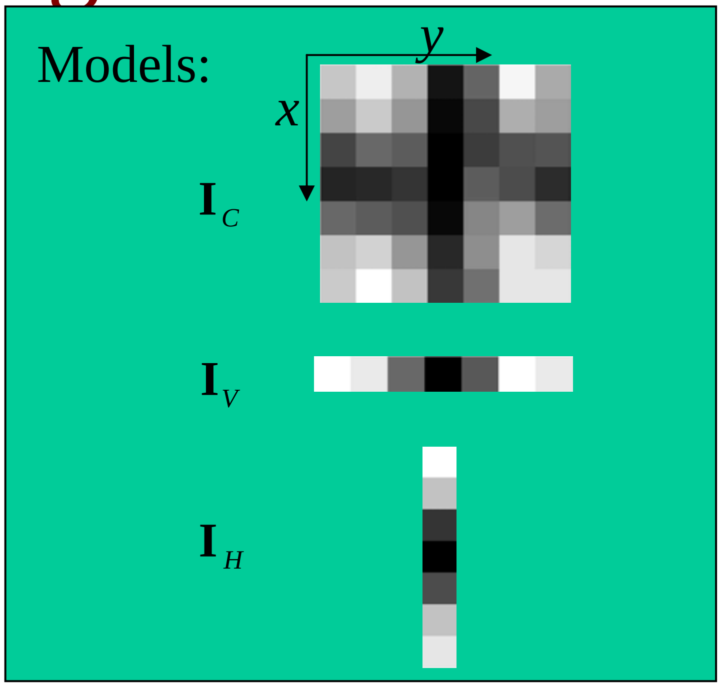

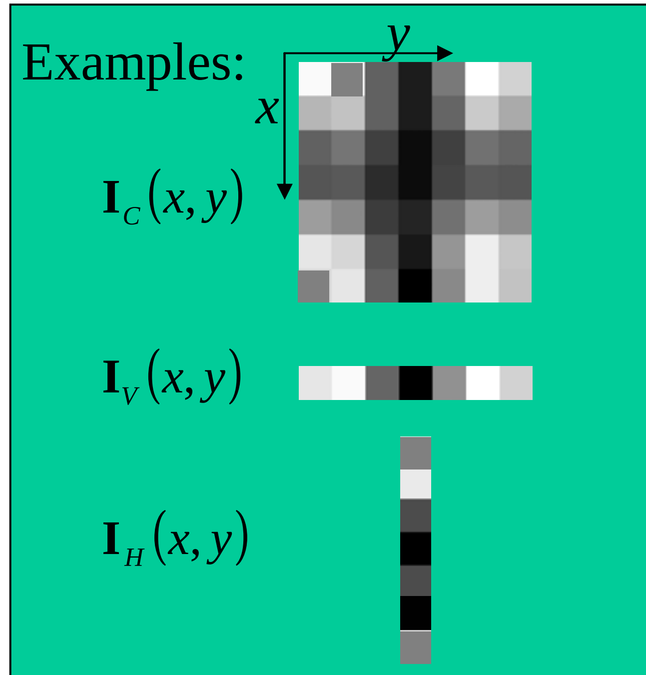

$$\mathbf{I}_V(x,y)=[I(x,y-3),\ldots,I(x,y),\ldots,I(x,y+3)]^T$$

$$\mathrm{dis}(\mathbf{I}_V(x,y),\mathbf{I}_V^T)=\sin\frac{\theta}{2}=\sqrt{\frac{1-\cos\theta}{2}}$$

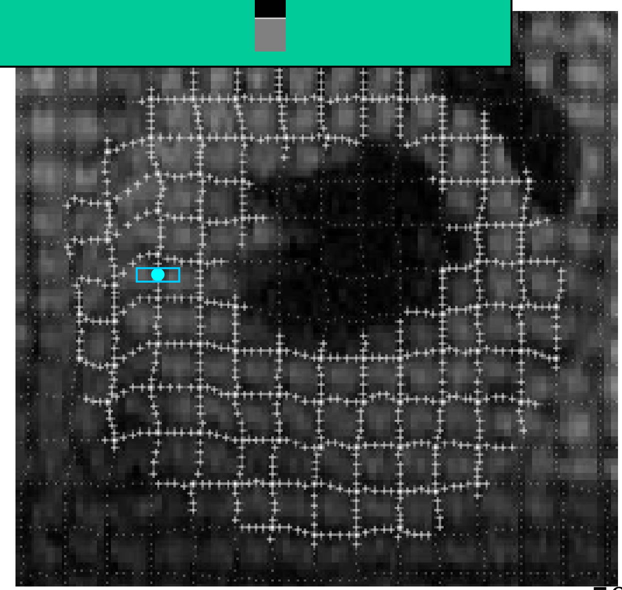

Tagline Detection: internal energy

- Energy functional: $E(\{x_{ij}, y_{ij}\}) = \sum_{(i,j)\in V}[\alpha_V E_{V\mathrm{int}}(x_{ij}, y_{ij}) + \beta_V D_V(x_{ij}, y_{ij})] + \sum_{(i,j)\in H}[\alpha_H E_{H\mathrm{int}}(x_{ij}, y_{ij}) + \beta_H D_H(x_{ij}, y_{ij})] + \sum_{(i,j)\in C}[\alpha_C E_{C\mathrm{int}}(x_{ij}, y_{ij}) + \beta_C D_C(x_{ij}, y_{ij})]$

- Control the smoothness of taglines

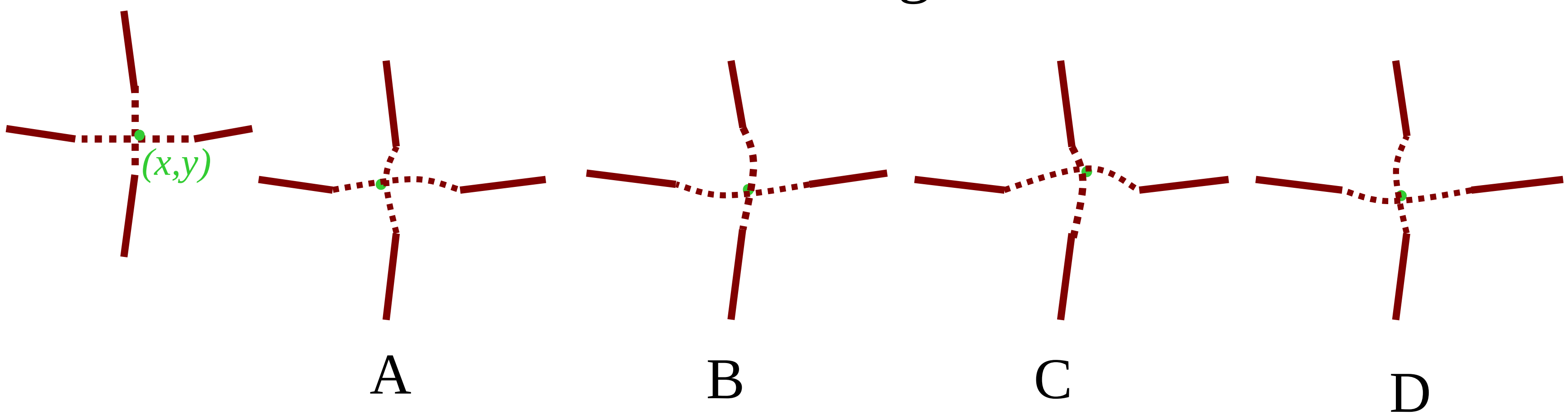

Left Ventricle Tagline Detection

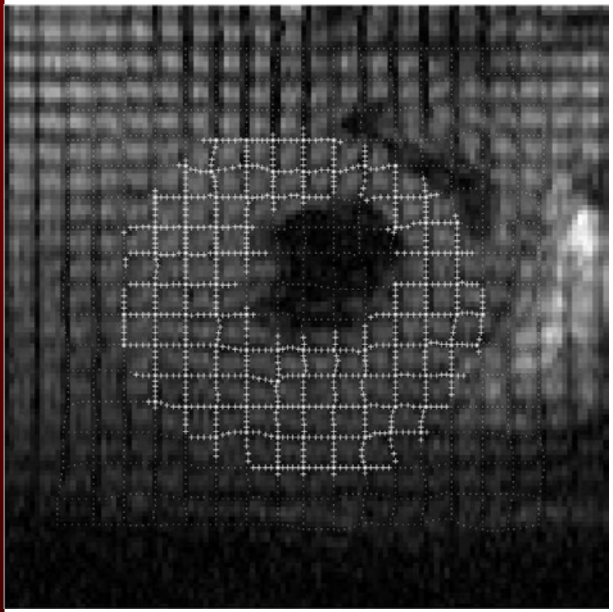

End of diastole

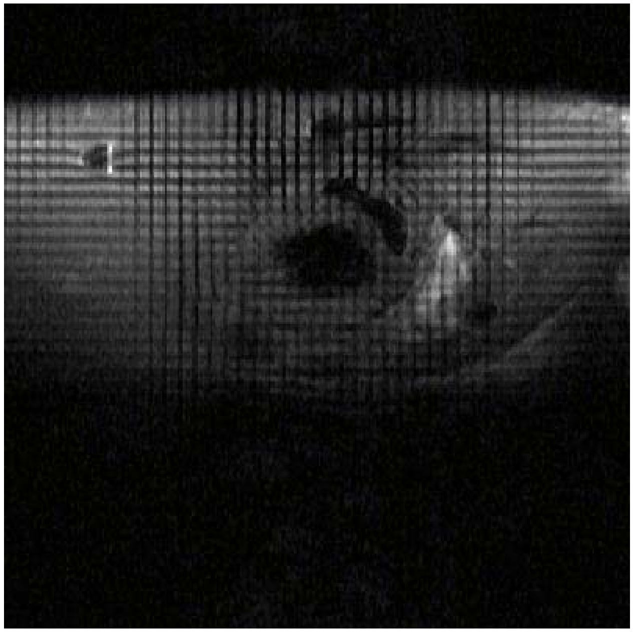

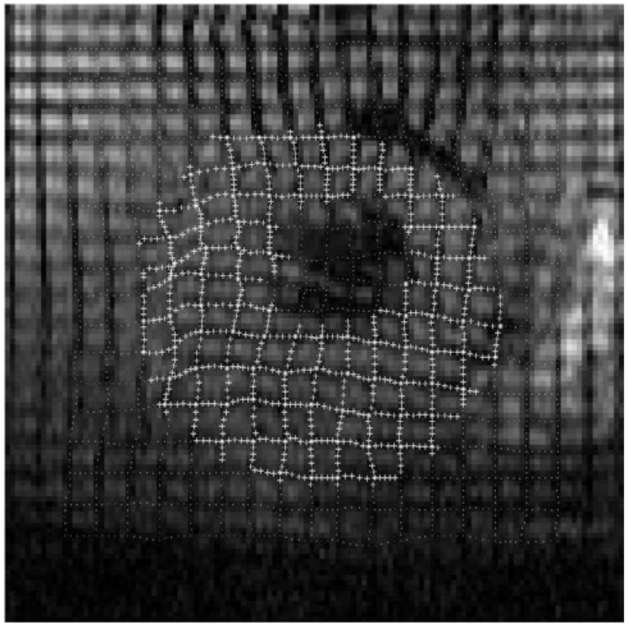

End of systole

Dense Displacement Field Estimation

- The displacement field of the myocardial pixels is estimated based on the displacement field of the taglines.

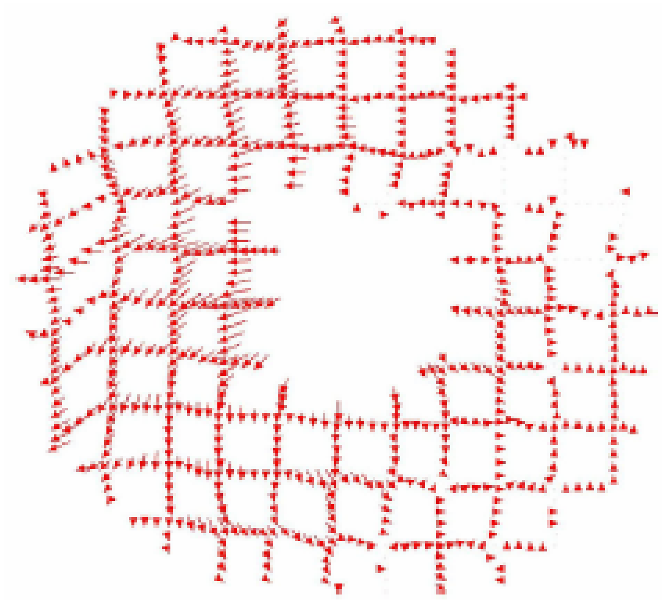

- An affine model, **A**(x,y), is used to describe the motion of the myocardium locally.

Affine Transform

- Determine the affine transform

$$\mathbf{S}=\begin{bmatrix} x_1 \cdots x_K \\ y_1 \cdots y_K \\ 1 \cdots 1 \end{bmatrix} \quad \mathbf{S'}=\begin{bmatrix} x_1^{'} & \cdots & x_K^{'} \\ y_1^{'} & \cdots & y_K^{'} \end{bmatrix} \quad \mathbf{A}=\begin{bmatrix} a_1 & a_2 & a_3 \\ a_4 & a_5 & a_6 \end{bmatrix}$$

$$\hat{\mathbf{A}} = \arg\min_{\mathbf{A}} \left\| \mathbf{S}' - \mathbf{AS} \right\|_F$$

(F: Frobenius norm)

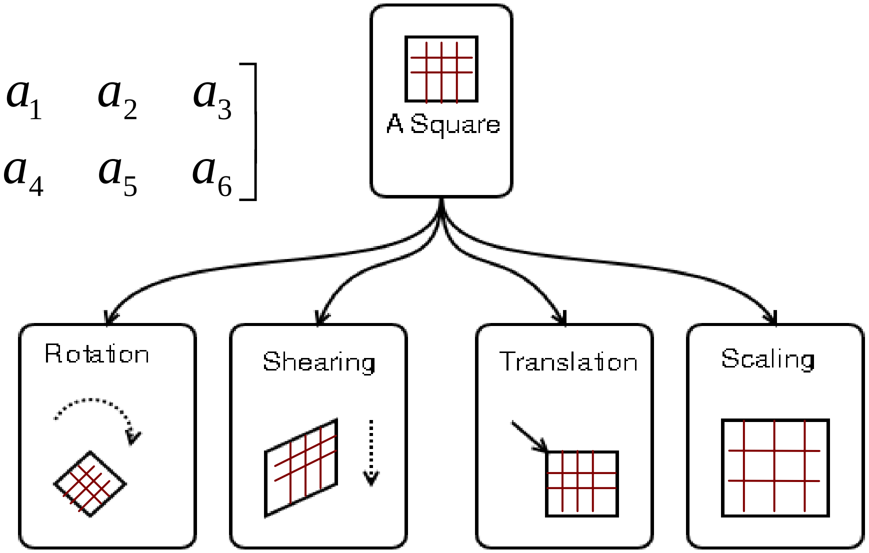

- Predict the coordinates of the pixel in the next frame by $\begin{bmatrix} x' \\ y' \end{bmatrix} = \mathbf{A}(x,y)\begin{bmatrix} x \\ y \\ 1 \end{bmatrix}$

Dense Motion Estimation

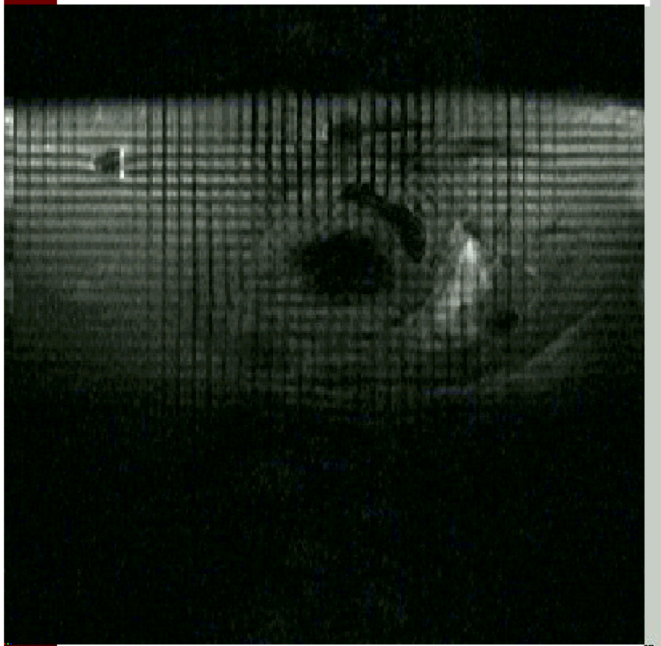

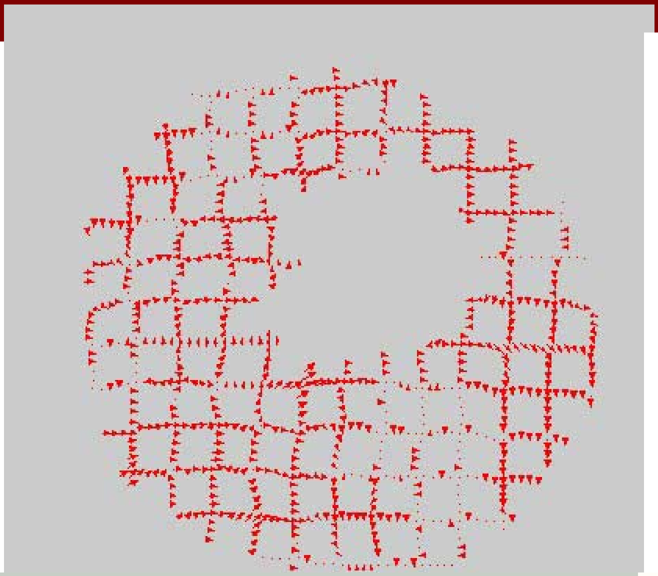

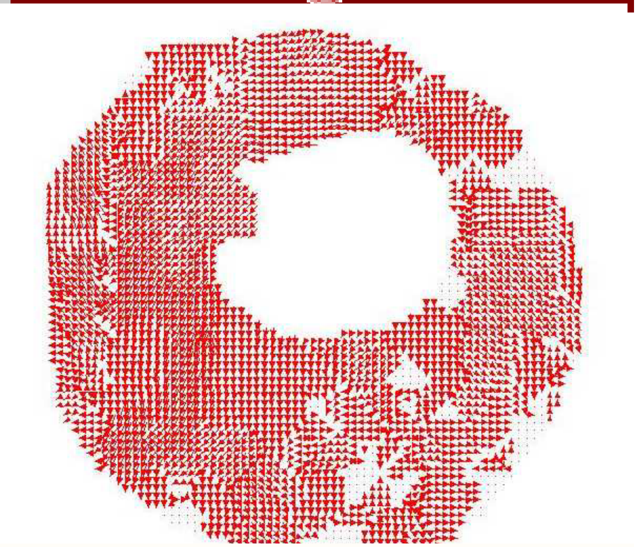

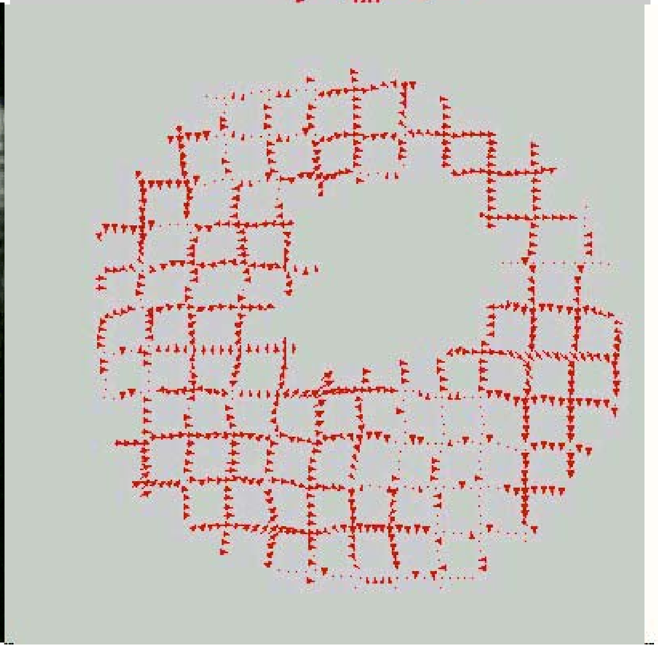

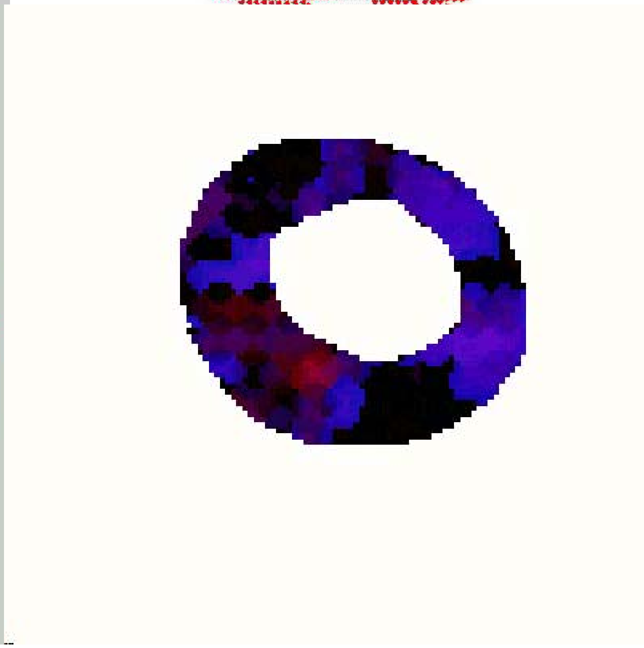

Tagline motion field
Displacement field

Pixel affine motion model
Dense motion field

Conclusions

- **Heart:**
  - **Automatic segmentation: Untagged MRI**
    - **Energy minimization stochastic active contour method segments heart and its structures**
  - **Motion detection: Tagged MRI**
    - **Energy minimization detects simultaneously *all* taglines.**
    - **Affine method estimates motion of *all* the myocardial pixels: dense motion estimate**
- **Kidney:**
  - **perfusion signal (automatic segmentation and organ monitoring)**
- **Future work:**
  - **monitor heart function by monitoring heart motion**
  - **3D: heart and kidney**

Bibliography

- Charnchai Pluempitiwiriyawej, José M. F. Moura, Yi-Jen L. Wu, Shinichi Kanno, and Chien Ho, "*Stochastic Active Contour for Cardiac MR Image Segmentation*," ***ICIP'03, IEEE International Conference on Image Processing***, Barcelona, Spain, September 2003.
- Ying Sun, Dewen Yang, Qing Ye, Chien Ho, and José M. F. Moura, "*Dense Motion Estimation in Tagged MRI Sequence*," ***Eleventh Scientific Meeting and Exhibition of the International Society for Magnetic Resonance in Medicine***, *ISMRM*, Toronto, ON, Canada, July 10-17, 2003.
- Ying Sun, Dewen Yang, Qing Ye, Mangay Williams, José M. F. Moura, Fernando Boada, Zhi-Pei Liang, and Chien Ho, "*Improving Spatiotemporal Resolution of USPIO Dynamic Imaging of Rat Kidneys*." in print, **Journal on Magnetic Resonance in Medicine**, November 2002. 13 pages.
- Qing Ye, Dewen Yang, Mangay Williams, Donald S. Williams, Charnchai Pluempitiwiriyawej, José M. F. Moura, and Chien Ho, "*In-vivo Detection of Acute Rat Renal Allograft Rejection by MRI with USPIO Particles*." **Kidney International**, 61:3, pp. 1124-1135, March 2002.
- Ying Sun, José M. F. Moura, Dewen Yang, and Chien Ho, "*Kidney segmentation in MRI Sequences Using Temporal Dynamics*," ***IEEE International Symposium on Bioimaging***, pp. 98-101, Washington DC, July, 2002.
- Ying Sun, Dewen Yang, Qing Ye, Chien Ho, and José M. F. Moura, "*Pseudo-Color Visualization of Dynamic Renal Perfusion in MRI*," ***Tenth Scientific Meeting and Exhibition of the International Society for Magnetic Resonance in Medicine***, *ISMRM*, Honolulu, Hawaii, May 19-24, 2002.
- Qing Ye, Dewen Yang, Ying Sun, Mangay Williams, Ben Y. Tseng, José M. F. Moura, and Chien Ho, "*Reduction of Renal Ischemia/ Reperfusion Injury Using Anti-Apoptosis Treatment with Pan-Caspase Inhibitor, MX1122*," **American Transplant Congress**, 2002.
- Dewen Yang, Qing Ye, Mangay Williams, Ying Sun, Tom C.-C. Hu, Donald S. Williams, José M. F. Moura, and Chien Ho, "*USPIO-Enhanced Dynamic MRI: Evaluation of Normal and Transplanted Rat Kidneys*." **Journal on Magnetic Resonance in Medicine**, 46:1152-1163, November 2001.